



DOEET147001

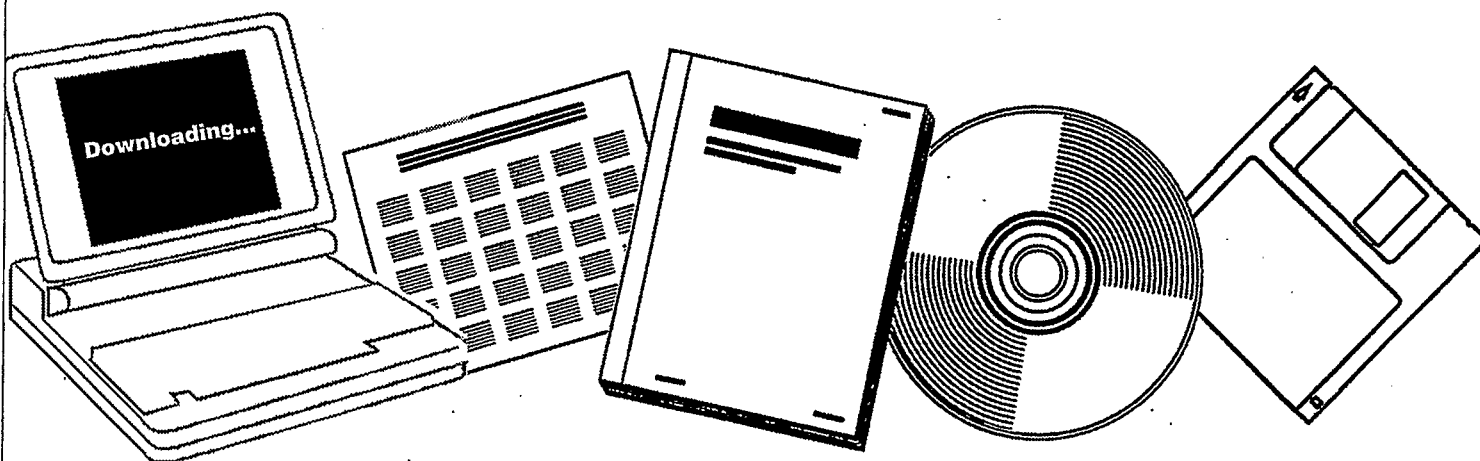
NTIS

One Source. One Search. One Solution.

**CHEMISTRY AND CATALYSIS OF COAL
LIQUEFACTION: CATALYTIC AND THERMAL
UPGRADING OF COAL LIQUID AND HYDROGENATION
OF CO TO PRODUCE FUELS. QUARTERLY PROGRESS
REPORT, OCTOBER-DECEMBER 1979**

UTAH UNIV., SALT LAKE CITY. DEPT. OF
MINING AND FUELS ENGINEERING

AUG 1980



U.S. Department of Commerce
National Technical Information Service

DOEET147001



DOE/ET/14700-1

Distribution Category UC-90d

Chemistry and Catalysis of Coal Liquefaction:
Catalytic and Thermal Upgrading of Coal Liquid
and Hydrogenation of CO to Produce Fuels

Quarterly Progress Report
for the Period Oct - Dec 1979

Dr. Wendell H. Wiser

University of Utah - Department of
Mining and Fuels Engineering
Salt Lake City, Utah 84112

Date Published - August 1980

Prepared for the United States Department
of Energy
Under Contract No. DE-AC01-79ET14700

CONTENTS

I	Cover Sheet	1
II	Objective and Scope of Work	3
III	Summary of Progress to Date	7
IV	Task 1 Chemical-Catalytic Studies	8
	Task 2 Carbon-13 NMR Investigation of CDL and Coal	10
	Task 3 Catalysis and Mechanism of Coal Liquefaction	12
	Task 4 Momentum, Heat and Mass Transfer in Co-Current Flow	13
	Task 5 The Fundamental Chemistry and Mechanism of Pyrolysis of Bituminous Coal	19
	Task 6 Catalytic Hydrogenation of CD Liquids and Related Polycyclic Aromatic Hydrocarbons	20
	Task 7 Denitrogenation and Deoxygenation of CD Liquids and Related N- and O- Compounds	29
	Task 8 Catalytic Cracking of Hydrogenated CD Liquids and Related Hydrogenated Compounds	34
	Task 9 Hydropyrolysis (Thermal Hydrocracking) of CD Liquids	Inactive
	Task 10 Systematic Structural-Activity Study of Supported Sulfide Catalysts for Coal Liquids Upgrading	Inactive
	Task 11 Basic Study of the Effects of Coke and Poisons on the Activity of Upgrading Catalysts	52
	Task 12 Diffusion of Polyaromatic Compounds in Amorphous Catalyst Supports	60
	Task 13 Catalyst Research and Development	65
	Task 14 Characterization of Catalysts and Mechanistic Studies	68
V	Conclusion	73

OBJECTIVE AND SCOPE OF WORK

I. The chemistry and Catalysis of Coal Liquefaction

Task 1 Chemical-Catalytic Studies

Coal will be reacted at subsoftening temperatures with selective reagents to break bridging linkages between clusters with minimal effect on residual organic clusters. The coal will be pretreated to increase surface area and then reacted at 25 to 350°C. Reagents and catalysts will be used which are selective so that the coal clusters are solubilized with as little further reaction as possible.

Task 2 Carbon-13 NMR Investigation of CDL and Coal

Carbon-13 NMR spectroscopy will be used to examine coal, coal derived liquids (CDL) and residues which have undergone subsoftening reactions in Task 1 and extraction. Improvements in NMR techniques, such as crosspolarization and magic angle spinning, will be applied. Model compounds will be included which are representative of structural units thought to be present in coal. Comparisons of spectra from native coals, CDL and residues will provide evidence for bondings which are broken by mild conditions.

Task 3 Catalysis and Mechanism of Coal Liquefaction

This fundamental study will gain an understanding of metal salt chemistry and catalysis in coal liquefaction through study of reactions known in organic chemistry. Zinc chloride and other catalytic materials will be tested as Friedel-Crafts catalysts and as redox catalysts using coals and selected model compounds. Zinc chloride, a weak Friedel-Crafts catalyst, will be used at conditions common to coal liquefaction to participate in well defined hydrogen transfer reactions. These experiments will be augmented by mechanistic studies of coal hydrogenation using high pressure thermogravimetric analysis and structural analysis. The results of these studies will be used to develop concepts of catalysis involved in coal liquefaction.

Task 4 Momentum Heat and Mass Transfer in CoCurrent Flow of Particle-Gas Systems for Coal Hydrogenation

A continuation of ongoing studies of heat and transport phenomena in cocurrent, co-gravity flow is planned for a one-year period. As time and development of existing work permits, the extension of this study to include a coiled reactor model will be undertaken. Mathematical models of coal hydrogenation systems will utilize correlations from these straight and coiled reactor configurations.

Task 5 The Fundamental Chemistry and Mechanism of Pyrolysis of Bituminous Coal

Previous work at the University of Utah indicates that coal pyrolysis, dissolution (in H-donor) and catalytic hydrogenation all have similar rates and activation energies. A few model compounds will be pyrolyzed in the range of 375 to 475°C. Activation energies, entropies and pro-

duct distributions will be determined. The reactions will assist in formulating the thermal reaction routes which also can occur during hydro-liquefaction.

II. Catalytic and Thermal Upgrading of Coal Liquids

Task 6 Catalytic Hydrogenation of CD Liquids and Related Polycyclic Aromatic Hydrocarbons

A variety of coal derived (CD) liquids will be hydrogenated with sulfided catalysts prepared in Task 10 from large pore, commercially available supports. The hydrogenation of these liquids will be systematically investigated as a function of catalyst structure and operating conditions. The effect of extent of hydrogenation will be the subject of study in subsequent tasks in which crackability and hydrolysis of the hydrogenated product will be determined. To provide an understanding of the chemistry involved, model polycyclic arenes will be utilized in hydrogenation studies. These studies and related model studies in Task 7 will be utilized to elucidate relationships between organic reactants and the structural-topographic characteristics of hydrogenation catalysts used in this work.

Task 7 Denitrogenation and Deoxygenation of CD Liquids and Related Nitrogen- and Oxygen-Containing Compounds

Removal of nitrogen and oxygen heteroatoms from CD liquids is an important upgrading step which must be accomplished to obtain fuels corresponding to those from petroleum sources. Using CD liquids as described in Task 6, exhaustive HDN and HDO will be sought through study of catalyst systems and operating conditions. As in Task 6, catalysts will be prepared in Task 10 and specificity for N- and O-removal will be optimized for the catalyst systems investigated. Model compounds will also be systematically hydrogenated using effective HDN/HDO catalysts. Kinetics and reaction pathways will be determined. A nonreductive denitrogenation system will be investigated using materials which undergo reversible nitridation. Conditions will be sought to cause minimal hydrogen consumption and little reaction of other reducible groups.

Task 8 Catalytic Cracking of Hydrogenated CD Liquids and Related Polycyclic Naphthenes and Naphthenoaromatics

Catalytic cracking of hydrogenated CD liquid feedstocks will be studied to evaluate this scheme as a means of upgrading CD liquids. Cracking kinetics and product distribution as a function of preceding hydrogenation will be evaluated to define upgrading combinations which require the minimal level of CD liquid aromatic saturation to achieve substantial heteroatom removal and high yields of cracked liquid products. Cracking catalysts to be considered for use in this task shall include conventional zeolite-containing catalysts and large-pore molecular sieve, CLS (cross-linked smectites) types under study at the University of Utah. Model compounds will be subjected to tests to develop a mechanistic understanding of the reactions of hydro CD liquids under catalytic cracking conditions.

Task 9 Hydropyrolysis (Thermal Hydrocracking) of CD Liquids

Heavy petroleum fractions can be thermally hydrocracked over a specific range of conditions to produce light liquid products without excessive hydrogenation occurring. This noncatalytic method will be applied to a variety of CD liquids and model compounds, as mentioned in Task 6, to determine the conditions necessary and the reactivity of these CD feedstocks with and without prior hydrogenation and to derive mechanism and reaction pathway information needed to gain an understanding of the hydropyrolysis reactions. Kinetics, coking tendencies and product compositions will be studied as a function of operating conditions.

Task 10 Systematic Structural-Activity Study of Supported Sulfide Catalysts for Coal Liquids Upgrading

This task will undertake catalyst preparation, characterization and measurement of activity and selectivity. The work proposed is a fundamental study of the relationship between the surface-structural properties of supported sulfide catalysts and their catalytic activities for various reactions desired. Catalysts will be prepared from commercially available supports composed of alumina, silica-alumina, silica-magnesia and silica-titania, modification of these supports to change acidity and to promote interaction with active catalytic components is planned. The active constituents will be selected from those which are effective in a sulfided state, including but not restricted to Mo, W, Ni and Co. The catalysts will be pre-sulfided before testing. Catalyst characterization will consist of physico-chemical property measurements and surface property measurements. Activity and selectivity tests will also be conducted using model compounds singly and in combination.

Task 11 Basic Study of the Effects of Coke and Poisons on the Activity of Upgrading Catalysts

This task will begin in the second year of the contract after suitable catalysts have been identified from Tasks 6, 7 and/or 10. Two commercial catalysts or one commercial catalyst and one catalyst prepared in Task 10 will be selected for a two-part study, (1) simulated laboratory poisoning/coking and (2) testing of realistically aged catalysts. Kinetics of hydrogenation, hydrodesulfurization, hydrodenitrogenation and hydrocracking will be determined before and after one or more stages of simulated coking. Selected model compounds will be used to measure detailed kinetics of the above reactions and to determine quantitatively how kinetic parameters change with the extent and type of poisoning/coking simulated. Realistically aged catalysts will be obtained from coal liquids upgrading experiments from other tasks in this program or from other laboratories conducting long-term upgrading studies. Deactivation will be assessed based on specific kinetics determined and selective poisoning studies will be made to determine characteristics of active sites remaining.

Task 12 Diffusion of Polyaromatic Compounds in Amorphous Catalyst Supports

If diffusion of a reactant species to the active sites of the catalyst is slow in comparison to the intrinsic rate of the surface reaction, then only sites near the exterior of the catalyst particles will be utilized effectively. A systematic study of the effect of molecular size on the sorptive diffusion kinetics relative to pore geometry will

be made using specific, large diameter aromatic molecules. Diffusion studies with narrow boiling range fractions of representative coal liquid will also be included. Experimental parameters for diffusion kinetic runs shall include aromatic diffusion model compounds, solvent effects, catalyst sorption properties, temperature and pressure.

III. Hydrogenation of CO to Produce Fuels

Task 13 Catalyst Research and Development

Studies with iron catalysts will concentrate on promoters, the use of supports and the effects of carbiding and nitriding. Promising promoters fall into two classes: (1) nonreducible metal oxides, such as CaO, K₂O, Al₂O₃ and MgO, and (2) partially reducible metal oxides which can be classified as co-catalysts, such as oxides of Mn, Mo, Ce, La, V, Re and rare earths. Possible catalyst supports include zeolites, alumina, silica, magnesia and high area carbons. Methods of producing active supported iron catalysts for CO hydrogenation will be investigated, such as development of shape selective catalysts which can provide control of product distribution. In view of the importance of temperature, alternative reactor systems (to fixed bed) will be investigated to attain better temperature control. Conditions will be used which give predominately lower molecular weight liquids and gaseous products.

Task 14 Characterization of Catalysts and Mechanistic Studies

Catalysts which show large differences in selectivity in Task 13 will be characterized as to surface and bulk properties. Differences in properties may provide the key to understanding why one catalyst is superior to another and identify critical properties, essential in selective catalysts. Factors relating to the surface mechanism of CO hydrogenation will also be investigated. Experiments are proposed to determine which catalysts form "surface" (reactive) carbon and the ability of these catalysts to exchange C and O of isotopically labelled CO. Reactions of CO and H₂ at temperatures below that required for CO dissociation are of particular interest.

Task 15 Completion of Previously Funded Studies and Exploratory Investigations

This task is included to provide for the orderly completion of coal liquefaction research underway in the expiring University of Utah contract, EX-76-C-01-2006.

III Summary of Progress to Date

Studies of the chemistry and catalysis of coal hydrogenation have been initiated with the construction of a flow reactor for extraction of coal and the development of analytical techniques. Work was initiated on the design of a rotor for ^{13}C nuclear magnetic resonance of solid coal and extracted coal. Studies on momentum, heat and mass transfer in a fluidized bed simulated conditions for coal hydrogenation and were used to investigate effects of particle size and solids loading.

The catalytic upgrading of coal-derived liquids is investigated by studies of the catalytic denitrogenation, desulfurization, deoxygenation and cracking of model compounds. Aging of Co-Mo catalysts was found to reduce the number of active sites but not the nature of the sites.

A Raney catalyst is being developed for the hydrogenation of carbon monoxide. Temperature programmed desorption was used to study the properties of an iron manganese oxide catalyst previously shown to give high yields of C_2 - C_{10} hydrocarbons.

Task 1

A Systematic Study of Coal Structure by Extraction Liquefaction Under Mild Reaction Conditions

Faculty Advisor: J. Shabtai
Graduate Student: H.B. Oblad

Introduction

This study is concerned with extractive coal liquefaction under mild experimental conditions, using a variety of solvents and homogenous catalysts. Coal slurries will be processed in a small integral flow reactor which will be operated at temperatures of 100-300°C, hydrogen pressures of 100-1000 psig and very short residence times. The mild conditions will be adjusted to obtain very low coal conversions, e.g., 2-5 percent to avoid secondary reactions. The slurry will be quenched, the liquids will be removed and analyzed, and the washed solids will be reloaded into the reactor with fresh solvent and catalyst. Repetition of this procedure coupled with the application of selective catalysts should yield relatively simple primary products. The information gathered should reveal the types of original structural components and interconnecting functional groups present in coal.

Project Status

A flow reactor has been constructed which is capable of pumping a dilute coal slurry through a preheater and a 2 zone furnace. The reactor tube can be heated up to $\approx 300^{\circ}\text{C}$ and hold pressures up to about 2000 psig. Coal slurries of 10 volume parts liquid to 1 weight part coal powder can be pumped at volumetric flow rates up to 6 cc/sec. They are pumped into a large bore preheater and then passed into a long, narrow bore coiled dissolver where it resides for approximately 6 sec. The residence time can be lengthened by decreasing the pumping rate. The bottom limit to the slurry flow rate is governed by the sedimentation rate of the coal particles in the preheater. Only coal 200 mesh and smaller can be used, thus avoiding plugging the reactor. The hot slurry is cooled rapidly in a concentric tube heat exchanger. Cold water is passed through the annular space between the 2 concentric tubes at very high velocity and in cocurrent flow. Quench is achieved in about 1 1/2 sec. The slurry can be recycled to the stirred feed hopper or can be expelled to a receiver.

A coal from the U.S. Fuel Mine in Utah has been recycled in the reactor. It is a high volatile bituminous b type coal. It was circulated first with cyclohexane for 7 hours. The slurry was pumped out of the reactor and separated in a centrifuge. The remaining coal was retrieved for further extraction. The liquid was decanted and the cyclohexane removed. The resin was weighed and subjected to various analyses. The same coal sample was then extracted in this manner 3 more times. The solvents used were benzene, acetone and tetrahydrofuran in that order. The extracts underwent analysis by infra-red spectroscopy, ^{13}C NMR spectroscopy, CHN elemental analysis and molecular weight determination by vapor pressure osmometry.

Extraction at 150°C and 250°C showed no significant difference in depth of extraction. Likewise variation of N₂ pressure (100-150 psig) had little effect on extraction except to maintain the solvents in a liquid or dense phase. The depth of extraction was in the same range as those reported earlier when performed by other methods.

Future Work

Coal samples will be pretreated by impregnation with different salts, followed by mild heating (150-300°C), for the purpose of increasing their internal surface area and pore volume. Such pretreated samples will be subjected to extractive liquefaction in the newly constructed reactor using (a) nonreacting solvents and (b) soluble catalyst-solvent systems.

Task 2

Carbon-13 NMR Investigation of CDL and Coal

Faculty Advisor: R.J. Pugmire
Post Doctoral: D.K. Dalling

Introduction

Carbon-13 NMR (CMR) spectroscopy can provide significant insights into the structure of solid coal by means of direct examination. In addition, comparison of solid coal spectra with that obtained from the corresponding residue and coal derived liquids provides a valuable new means for exploring the details of the chemistry of the coal liquefaction process. The effect of strong dipolar fields in the solid together with the large chemical shift anisotropy of aromatic carbons in the solid state combine to limit the availability of the extensive detail common in liquid spectra. The C-H dipolar interaction can produce ^{13}C linewidths of up to 40 KHz while the chemical shift anisotropy can be as large as several KHz even at moderate field strengths. The detection of a nucleus of low natural abundance (e.g., ^{13}C at 1.1%) presents sensitivity problems in crystalline solids that are also challenging. Recently, developed experimental techniques now provide powerful methods for investigating the intricate structural details in solid coal. The use of high power proton polarization techniques can be used to reduce the dipolar broadening arising from C-H interactions while rapid magic angle spinning reduces not only the dipolar broadening but also the chemical shift anisotropy of the resonance lines. The combination of these two experimental techniques produces lines of 3-50 Hz width at a half height depending upon the spectral and operating parameters. Work under this task will attempt to improve on these experimental techniques and apply them to the measurement of solid coal, coal liquids and model compounds.

Project Status

During the first quarter, work was initiated at a modest level on examining alternative designs for magic angle spinning (MAS) rotors. Ideas were formulated for redesign of the present MAS spinners to achieve high speed (5-6 KHz) stable spinning capability of larger rotors than those presently in use in this laboratory. Material considerations (in addition to design criteria) are very important for two reasons: 1) The material used for rotor construction must have sufficient strength so as not to deform the rotor at high spinning rates. Work on model compounds indicated that even minor spinner instability can give rise to small spinning side bands. Furthermore, at high spinning rates some rotors have exploded. 2) To cut down the amount of time required to obtain data on a given solid, one must increase the amount of sample inside the receiver coil. Hence, the need for larger rotors. Several larger rotors have been built to spin approximately 200 mg of sample as opposed to the 100 mg normally used in the past. If this effort is successful, the instrument time required to achieve a given S/N ratio will be reduced by a factor of 4.

Future Work

The ^{13}C NMR analysis of coal liquids obtained by ZnCl_2 catalyzed hydrogenation of coals at short contact time will be initiated.

Task 3

Catalysis and Mechanism of Coal Liquefaction

Faculty Advisor: D.M. Bodily
Graduate Student: Jason Miller

Introduction

The hydroliquefaction of coal may be characterized by a mechanism which involves the initial rupture of covalent bonds to form reactive intermediates. These intermediates may be stabilized by hydrogen transfer to form lower molecular weight products or they may polymerize to form insoluble char or coke. Metal halides such as zinc chloride have been shown to be active in the bond scission stage of the reaction where as many catalysts are active only in stabilizing the intermediates, often by regenerating a hydrogen donor. The combination of thermal and catalytic reactions occurring simultaneously results in a complicated reaction mechanism. The chemistry of $ZnCl_2$ will be studied with model compounds and coal by such reactions as hydrogen transfers, cleavage of specific bonds and interaction with π electron systems.

A high performance liquid chromatograph, HPLC, will be used to analyze liquid products of the reactions under study. Further characterization of the products will be by nuclear magnetic resonance, NMR, structural analysis and vapor pressure osmometry.

Project Status

Review of data obtained under a previous contract leads to the conclusion that zinc chloride is an active catalyst for bond scission in coal hydrogenation during the initial stage of the reaction. Solid catalysts such as cobalt molybdate or ferric oxide are ineffective below 20% conversion. Structural analysis of the initial products of hydrogenation with these catalysts indicates a higher hydrogen content, lower heteroatom content and lower aromaticity than the products at higher conversion. The structures are the same as those obtaining from samples hydrogenated with no catalyst. For impregnated zinc chloride catalyst, the structure of the liquids is quite different.

Future Work

An HPLC method for rapid analysis of coal hydroliquefaction products will be developed.

Task 4

Momentum, Heat and Mass Transfer in Cocurrent Flow

Faculty Advisor: J.D. Seader
Graduate Student: B.S. Brewster

Introduction

This project is concerned with an investigation of the momentum and heat transport phenomenon for gas-solids suspensions flowing vertically downward through a heated tube. The research is motivated by the lack of data or correlations thereof in the literature to the downward cocurrent configuration and a comparison to the upward cocurrent configuration. Both have application to coal-conversion reactors.

Project Status

During this period, heat transfer measurements were completed for the cocurrent downward flow of the coal particle-air system.

Initially, heat transfer measurements with air alone were conducted to determine the heat loss correction to be applied to subsequent measurements with coal suspensions. The air alone Nusselt numbers were also compared with standard correlations to check the system operability. Exit gas temperature profiles, measured in a few runs with coal suspensions, were used to determine the rate of gas-to-particle heat transfer in terms of an average particle Nusselt number for the suspension based on the particle-surface-area. Particle Nusselt numbers calculated from the data were then correlated in terms of average particle size, gas flow rate and solids loading; and the resulting correlations were used to calculate one-dimensional temperature profiles of the gas and solids. The gas temperature profile was then used to calculate the local wall Nusselt number. This was based on the total rate of heat transfer to the suspension and the temperature difference between the inside surface of the tube wall and the bulk gas.

Following a procedure developed by Kim, as reported earlier, heat loss from the heat transfer test section was essentially independent of gas mass flow rate and equal to a value that represented less than 5 percent of the total heat generated for most of the subsequent runs with coal suspensions.

Wall Nusselt numbers for the flow of air alone were obtained over a Reynolds number range of about 10000 to 30000. The data were in excellent agreement with the well-accepted correlations of Sparrow and Kays.

Using the measured heat loss, values of the heat flux at the inside surface of the tube, during studies with coal suspensions, were assumed to be uniform and were calculated from the total heat generated in the tube as measured electrically. The heat flux with coal suspensions was always higher than with air alone at the same gas flow rate. Data for three air flow rates are shown in Fig 1. At the high flow rate

($Re_{sg,av} \approx 29500$), the heat flux with 100-micron particles is higher than with 300-micron particles at solids loading ratios less than 3. This is due to the higher surface area for gas-to-particle heat transfer and, consequently, higher uptake of heat by the solid phase with the smaller particles. The data for $Re_{sg,av}$ equal to approximately 14100 show a higher heat flux with the smaller particles at solids loading ratios less than 3 and an approximately equal heat flux for both particle sizes at solids loading ratios greater than 5.

An upstream thermocouple was used to measure exit gas temperature for the tests with 100-micron coal suspension. The thermocouple indicated temperatures higher than the gas temperature due to heating of the probe by impacting particles. The magnitude of the impact heating was measured and correlated for temperature correction in terms of radial position, solids flow rate and gas velocity. Impact heating with the downstream probe in 300-micron suspensions was negligible, and no correction was necessary.

Complete radial profiles of the exit gas temperature for runs with coal suspensions were made for a number of runs. In every case, the gas temperature was decreased by the addition of solids due to the absorption of heat by the solids from the gas.

Bulk gas temperature was calculated by neglecting the effect of the solids on the shape of the gas velocity profile in the suspension and integrating the measured temperature profiles. The average particle Nusselt number in coal suspensions was based on the average particle-surface-area diameter of the suspension and calculated so as to make the predicted exit bulk gas temperature agree with that calculated from the measured profiles. These average particle Nusselt numbers are plotted in Fig 2, where they are seen to depend on gas flow rate, solids loading and particle size. Values for the 300-micron suspension are 2 to 10 times higher than those for the 100-micron suspension, consistent with the fact that the average surface-area-diameter of the larger particles is approximately three times that of the smaller particles. The particle Nusselt number increases with increasing flow rate and turbulence level of the gas, decreases with increasing solids loading ratio and at high loadings can be lower than the theoretical value of 2 for a sphere in an infinite stagnant fluid.

Particle Nusselt numbers were then used to calculate the solids and gas axial temperature profiles. Local wall Nusselt numbers for the suspension were then calculated from the wall temperature and these bulk gas temperature profiles, where gas properties were evaluated at the average of the inlet and outlet conditions. The resulting asymptotic Nusselt number (measured at a distance of 42 inches from the inlet of the heated tube) is compared with the correlations obtained with glass beads by Kim in Fig 3. The same trends observed with the glass bead suspensions are also apparent in the coal particle suspensions; i.e., Nusselt number is almost constant at the lower gas Reynolds numbers (9600 and 14200) and decreases only slightly with solids loading at the higher Reynolds number (28500).

Bulk gas and solids temperatures at the heat transfer section outlet were determined from the Nusselt number correlations. These resulting profiles led to the following observations. First, the temperatures of

both solids and gas decrease with increasing solids loading as previously observed with the gas temperature profiles. Second, the difference in temperature between the solids and gas is always greater with the larger size particles. Third, the outlet temperature of the solids in the 300-micron suspension is much less dependent on solids loading than that of the solids in the 100-micron suspension. Fourth, the outlet temperature of the solids is much higher in the 100-micron suspension than that of the solids of the 300-micron suspension at low solids loadings, but solids temperature in both suspensions appears to approach the same asymptotic value at high loadings.

Future Work

As discussed in previous progress reports, experimental results for cocurrent upward flow scatter widely and, thus, cannot be directly compared to the data obtained here for cocurrent downward flow. Accordingly, it is planned to modify the apparatus to conduct a limited number of runs in the upward flow configuration so that a comparison can be made.

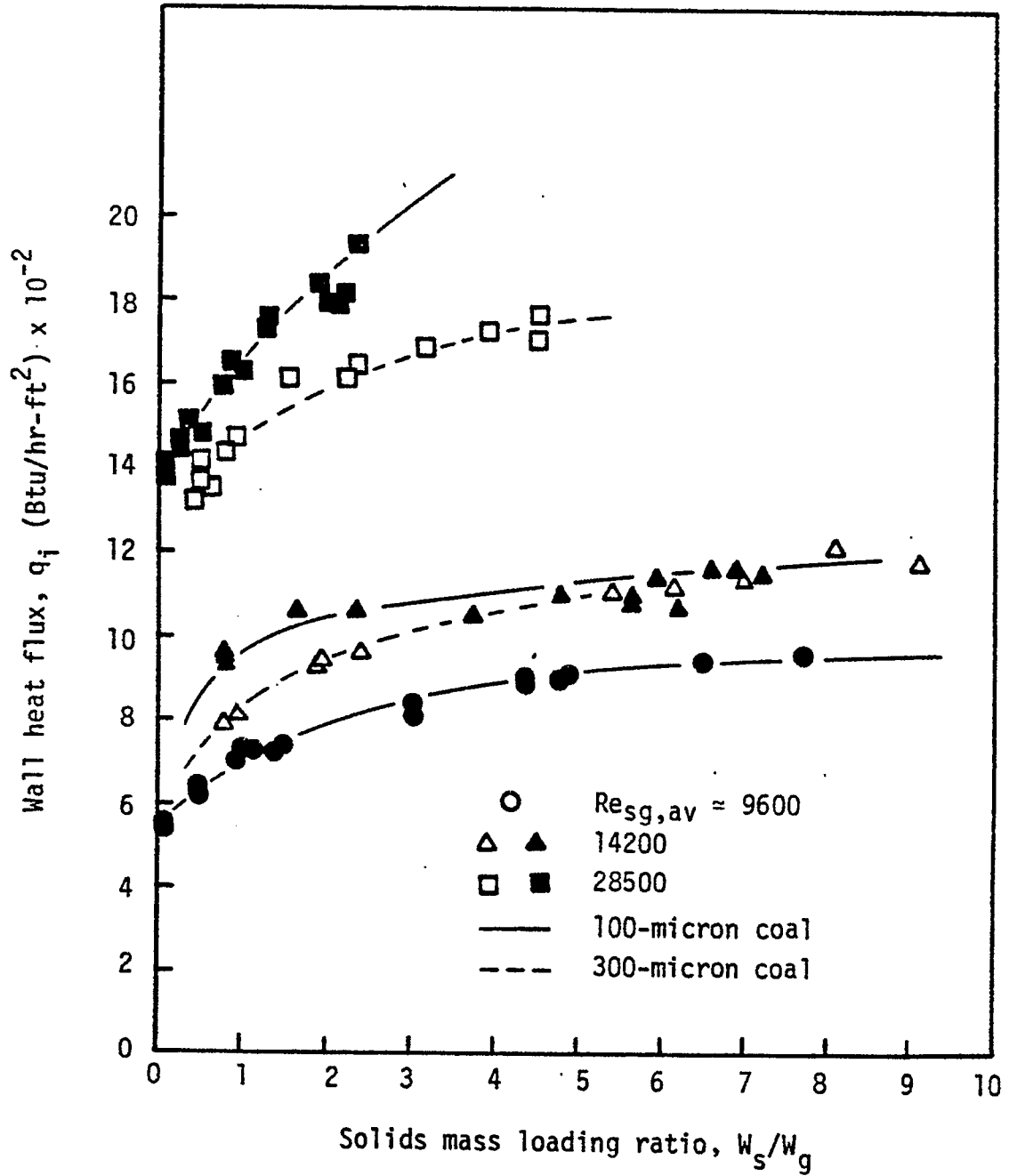


Fig. 1 Wall heat flux for coal suspensions

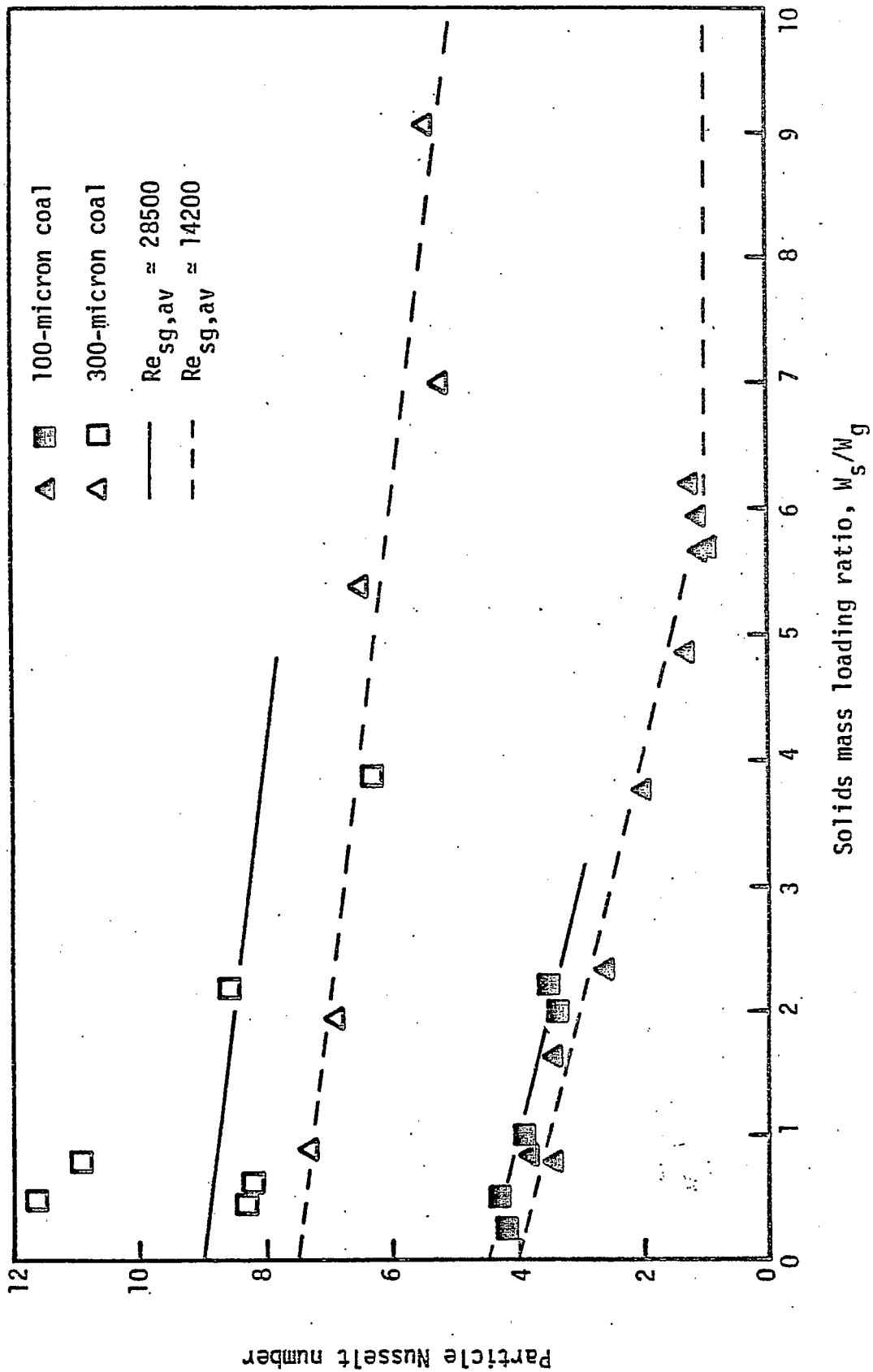


Fig. 2 Particle Nusselt number for coal suspensions

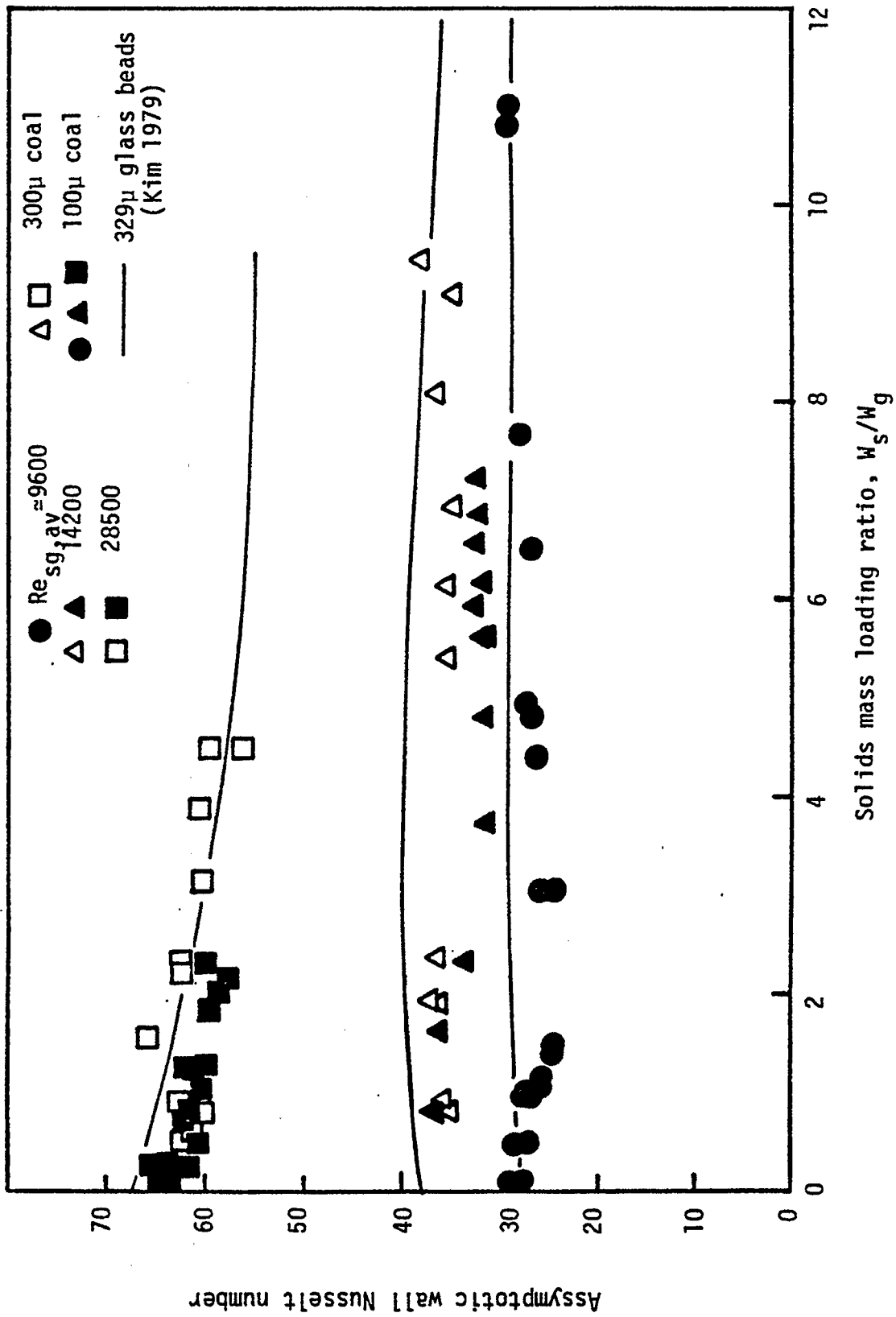


Fig. 3 Asymptotic wall Nusselt number for coal suspensions

Task 5

The Mechanism of Pyrolysis of Bituminous Coal

Faculty Advisor: W.H. Wiser
Graduate Student: John K. Shigley

Introduction

In the present state of knowledge concerning the fundamental chemistry of coal liquefaction, the liquefaction reactions are initiated by thermal rupture of bonds in the "bridges" joining configurations in the coal, yielding free radicals. The different approaches to liquefaction, except for Fischer-Tropsch variations, represent ways of stabilizing the free radicals to produce molecules. The stabilization involving abstraction by the free radicals of hydrogen from the hydroaromatic structures of the coal is believed to be the predominant means of yielding liquid size molecules in the early stages of all coal liquefaction processes, except Fischer-Tropsch variations. The objective of this research is to understand the chemistry of this pyrolytic operation using coal model compounds.

Project Status

One model compound has been received and the second one is currently being synthesized by Parrish Chemical Company of Provo, Utah.¹

The Perkin-Elmer thermogravimetric system has been calibrated and tested. Several preliminary experiments have been conducted on the first model compound using about 10 mg of the compound for each experiment. The preliminary thermogravimetric experiments indicate that the compound has too high a vapor pressure in the temperature range of interest (300-500°C) to be studied by this method. Preliminary indications from Parrish Chemical Company are that the second model compound will behave in a similar manner. It is, therefore, necessary to devise a new method to conduct the experimentation. A literature search is being conducted on current techniques for studying the pyrolysis of volatile compounds.

Future Work

A new method for studying the pyrolysis of the model compounds will be designed. It will be built, assembled, tested and used to determine the mechanism and kinetics of the model compounds.

References

1. W.H. Wiser et al., DOE Contract No. E (49-18)-2006, Quarterly Progress Report, Salt Lake City, Utah, Jan - Mar 1979.

Task 6

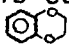
Catalytic Hydrodeoxygenation of Coal-Derived Liquids and Related Oxygen-Containing Compounds

Faculty Advisors: J. Shabtai
A. G. Oblad
Graduate Student: G. Haider

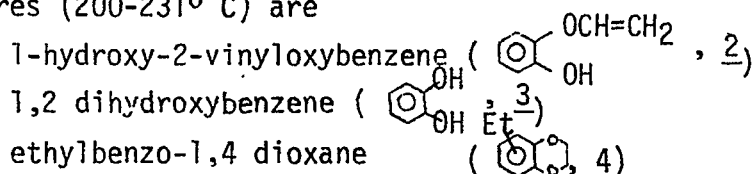
Introduction

Coal-derived liquids are characterized by the presence of a significant concentration of oxygen-containing components. Therefore, a systematic catalytic hydrodeoxygenation (HDO) study of coal-derived liquids and related model compounds is being carried out. The study provides information not only on the mechanism of HDO as related to catalytic upgrading of coal liquids, but also on the role of oxygen-containing compounds in primary coal liquefaction processes.

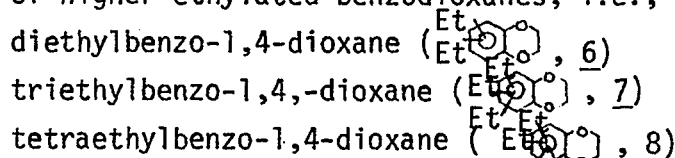
Project Status

The present report is concerned with a study of the hydrodeoxygenation of 1,4-benzodioxane (1, ). Figures 1 (A and B) and 2 (A and B) summarize the change in product composition from HDO of compound 1 as a function of temperature, using sulfided Ni-W/Al₂O₃ and sulfided Co-Mo/Al₂O₃ catalysts, respectively. For clarity in presentation, the change in product composition is subdivided into two sets (A and B), both in Figures 1 and 2. The Ni-W/Al₂O₃ and Co-Mo/Al₂O₃ catalyst precursors used were Sphericat 550 (1/16") and Nalcom 471 (1/32"), respectively. Both were supplied by Nalco Chemical Co.

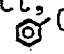
As seen from Figure 1 (A), the main products from compound 1 at low temperatures (200-231° C) are



Extrapolation to temperatures below 200°C indicates that the main product under such conditions is 2. With increase in temperature above 200°C, there is a gradual decrease in the concentration of 2, while the concentrations of 3 (found mostly as a polymer) and 4 gradually increase. After reaching a maximum around 260°C, the concentration of 3 slowly decreases at higher temperatures. However, compound 4, after passing through a maximum around 230°C gradually decreases between 230-350°C. This is accompanied by the formation of higher ethylated benzodioxanes, i.e.,



especially between 290 - 350°C. For simplicity the ethylated dioxanes 6, 7 and 8 have been plotted together in Figure 1-A. At temperatures above 260°C

(Figure 1-B) there is also some formation of ethylphenol (9), diethylphenol (10) and triethylphenol (11). Above 290°C the product contains small amounts of cyclohexane (12) and methylcyclopentane (14), and another product, tentatively assigned the structure of 1-hydroxy-2-benzoxyethylene (, 15). Similar compositional change patterns are observed with a sulfided Co-Mo/Al₂O₃ catalyst (Figures 2-A and 2-B), although there are some significant differences. In particular, a marked increase in the rate of formation of phenol (5), apparently by hydrodeoxygenation of compounds 2 and 3, is observed with the sulfided Co-Mo/Al₂O₃ catalyst (Figure 2-A). It is also observed that with this catalyst the concentrations of benzene (16) and cyclohexene are somewhat higher than those found in the reaction product using the sulfided Ni-W/Al₂O₃ catalyst. Compound 2 (1-hydroxy-2-vinyloxybenzene) could not be observed even at 200°C. It is possible that 2 is formed initially, but then converted into 3 and 5 at a much faster rate than that observed in the reaction with the sulfided Ni-W/Al₂O₃ catalyst (compare with Fig 1-A). Another interesting difference is that at 200-230°C, the product with Co-Mo/Al₂O₃ catalyst contains some ethanol (17), which might be derived by a two-step hydrogenolysis sequence directly from the feed 1 (vide infra).

The results in Figures 1(A and B) and 2(A and B) can be rationalized by considering the mechanistic schemes outlined in Figures 3 and 4. In the reaction with the sulfided Ni-W/Al₂O₃ catalyst (Fig 3) 1,4-benzodioxane (1) apparently undergoes fast dehydrogenation to dehydrobenzodioxane (18) which by hydrogenolytic cleavage yields Compound 2. Hydrogenolysis of 2 gives ethylene and 1,2-dihydroxybenzene over sulfided catalysts have been indicated in previous studies.^{1,2} The presence of ethanol in the reaction product with the sulfided Co-Mo/Al₂O₃ catalyst (Fig 2-A) indicates that there is apparently an additional pathway leading to the formation of phenol (5), viz., hydrogenolysis of 1 to the intermediate alcohol 22, followed by hydrogenolysis of 22 to yield 5 and ethanol, which could be consumed as an alkylating agent (Fig 4).

The present study indicates that certain reaction pathways in the HDO of ortho-diphenolic ethers, e.g., 1,4-benzodioxane or 1,2-dialkoxybenzenes, produce upon hydrogenolysis reactive coke precursors, e.g., 0-dihydroxybenzene. This is an additional evidence (see also previous report) that oxygen-containing components of coal liquids could play a major role in the fast deactivation of conventional sulfided catalysts in the upgrading processes.

Identification of products from HDO of 1,4-benzodioxane (1) was carried out by gas chromatography/mass spectrometry and by comparison with reference samples. A typical gas chromatogram of products from HDO of 1 is shown in Figure 5.

Future Work

Systematic HDO studies are being presently carried out with the ester.

References

1. A. Dierichs and R. Kubicka, Fenoly a zasady z uhli (Phenols and Bases from Coal) SNTL, Prague, 1956.
2. O. Weisser and S. Landa, "Sulfide Catalysts, Their Properties and Applications," Pergamon Press, New York, New York, 1973.

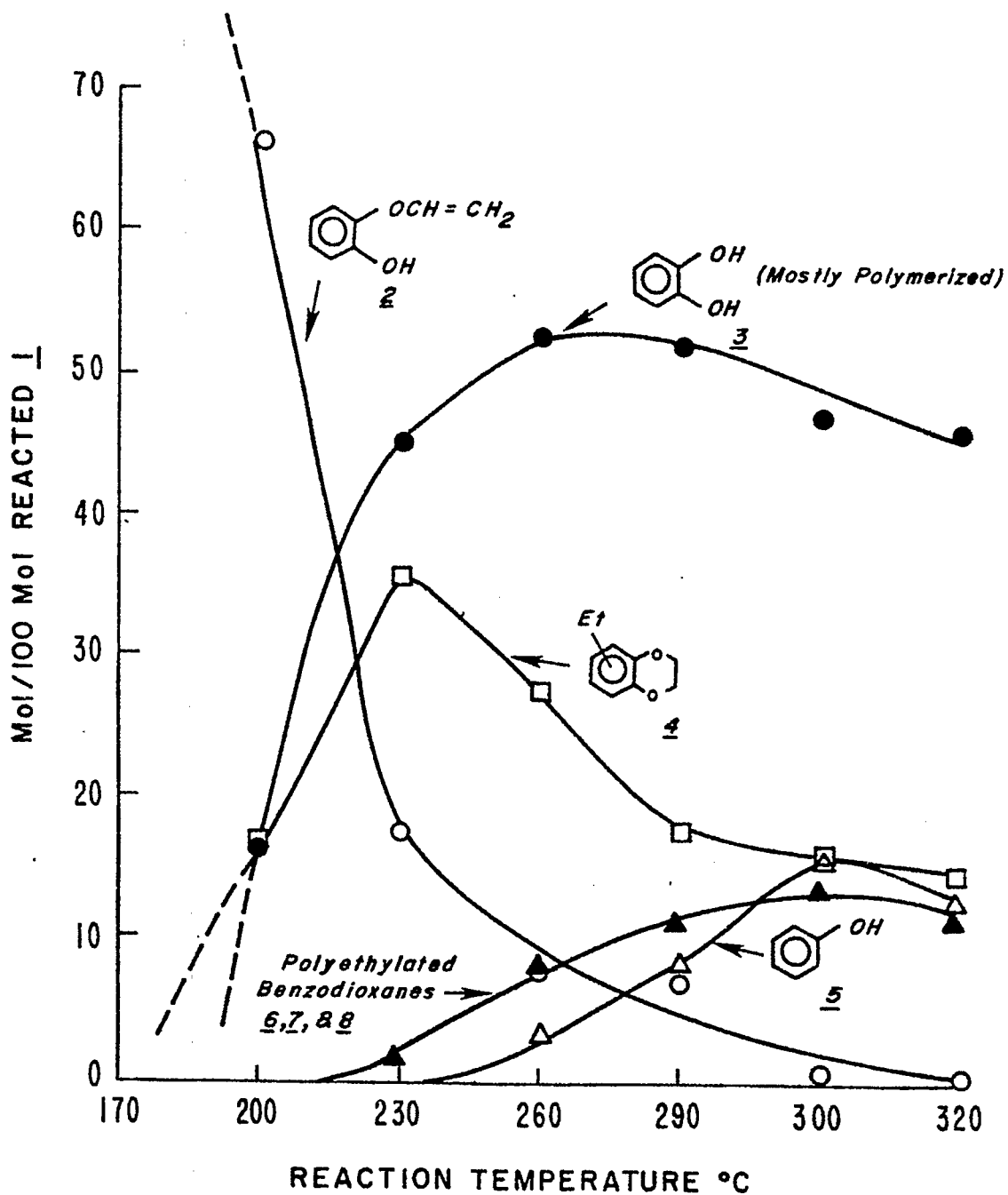


Figure 1-A. Change in composition of product from hydrodeoxygenation of 1,4-benzodioxane (1) as a function of temperature (pressure: 1550 psig; reaction time: 1 hr; catalyst: sulfided Ni-W/Al₂O₃).

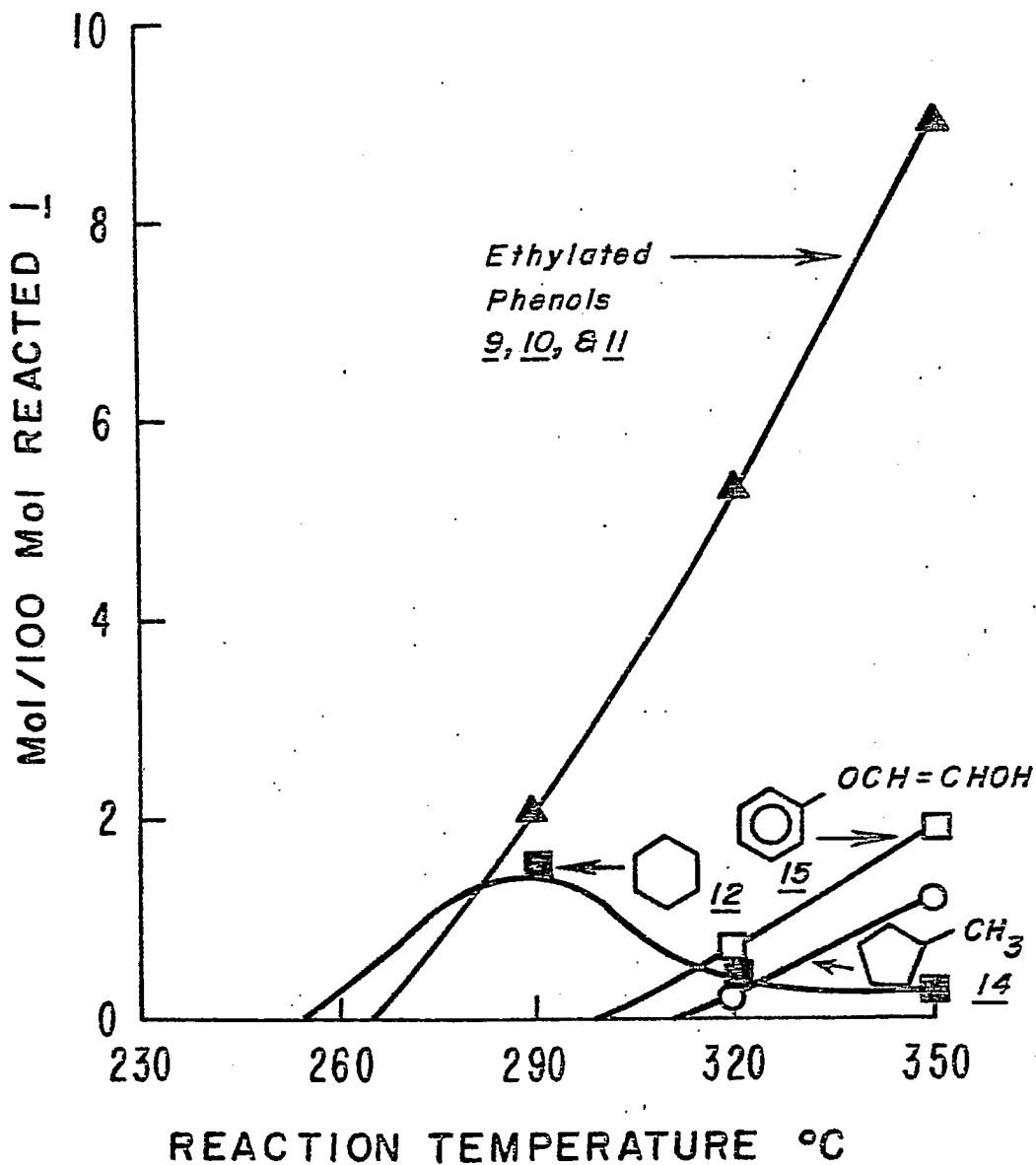


Figure 1-B. Change in composition of product from hydrodeoxygenation of 1,4-benzodioxane (I) as a function of temperature (pressure: 1550 psig; reaction time: 1 hr; catalyst: sulfided Ni-W/Al₂O₃).

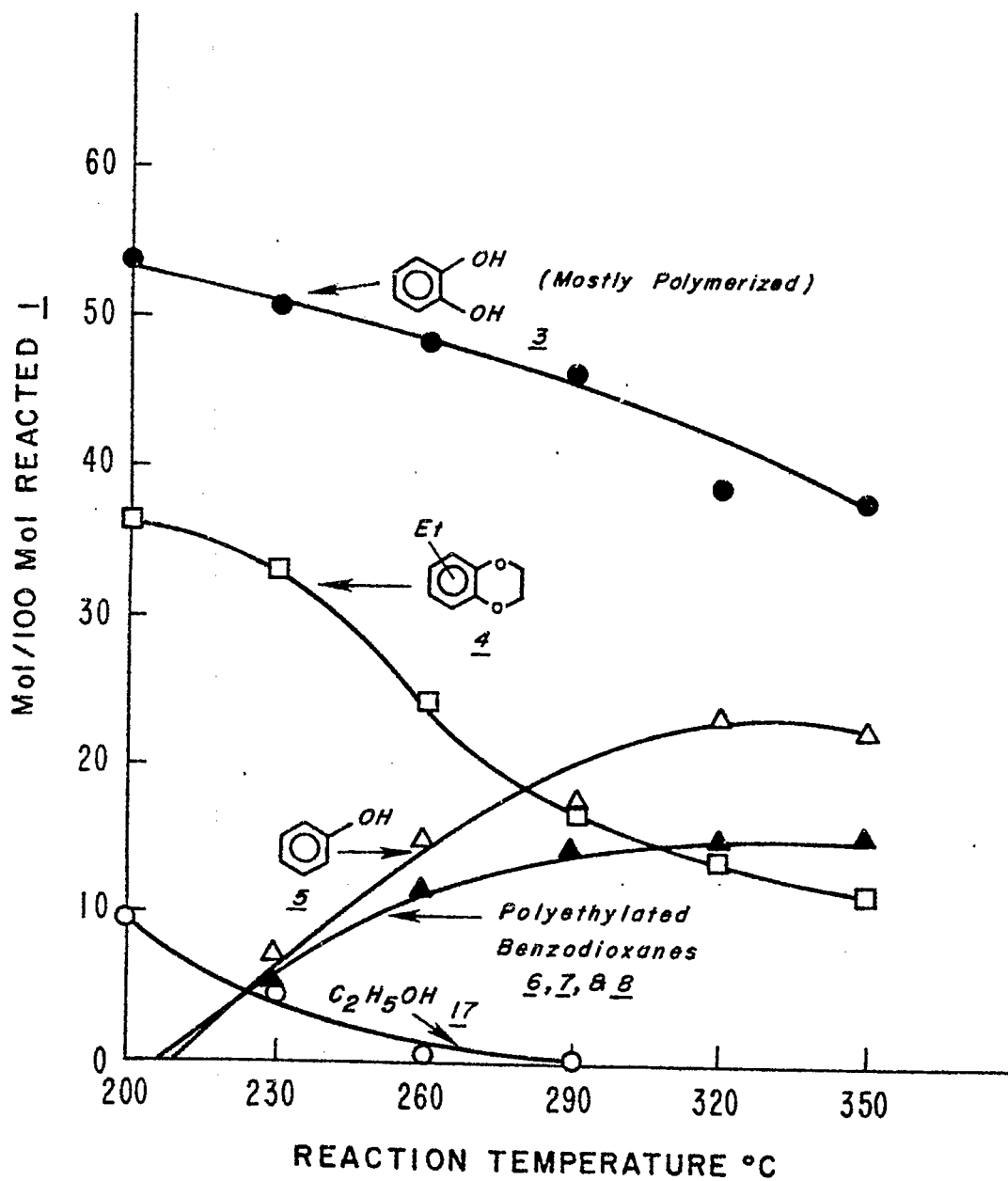


Figure 2-A. Change in composition of product from hydrodeoxygenation of 1,4-benzodioxane (1) as a function of temperature (pressure: 1550 psig; reaction time: 1 hr; catalyst: sulfided Co-Mo/Al₂O₃).

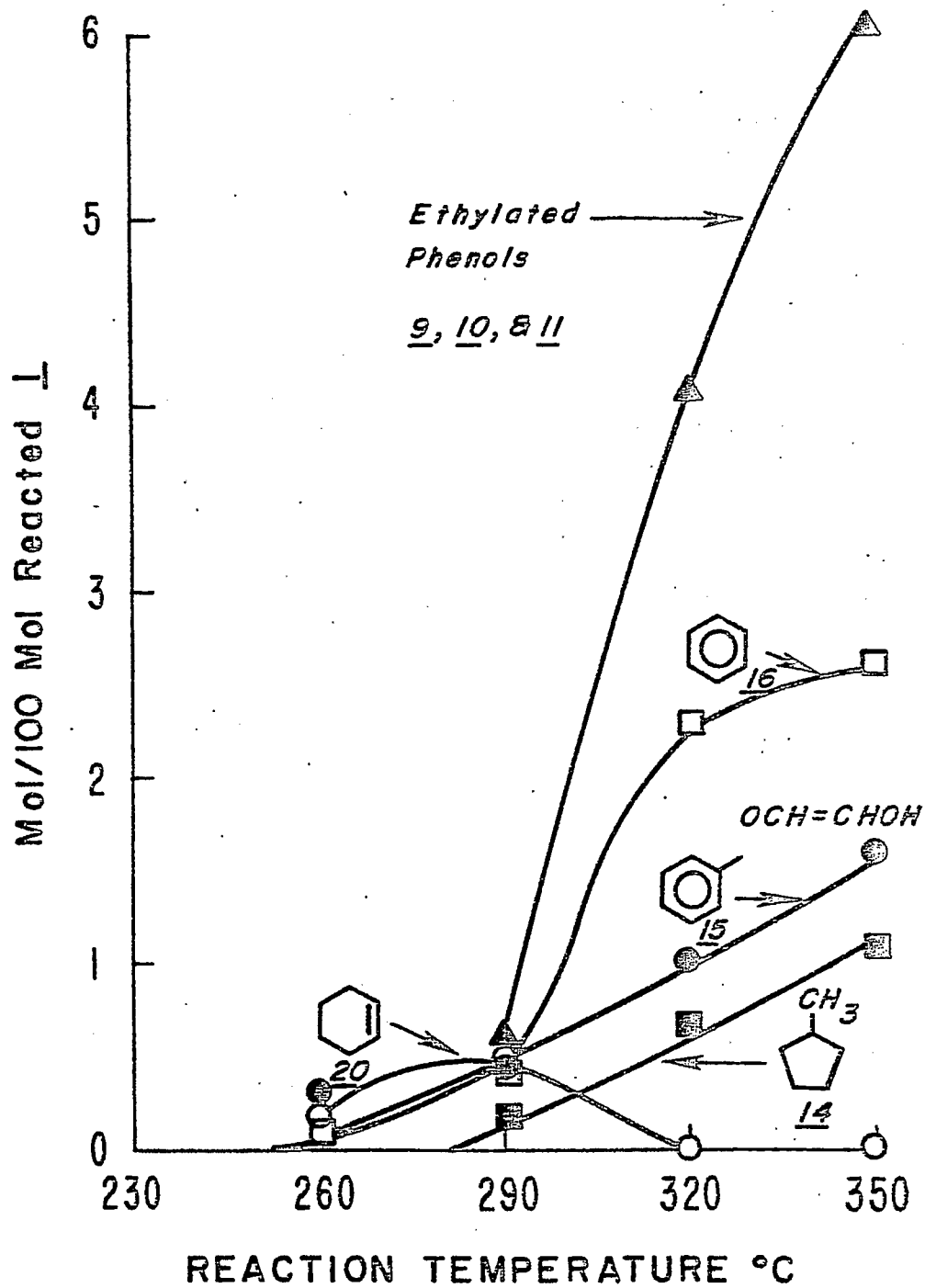


Figure 2-B. Change in composition of product from hydrodeoxygenation of 1,4-benzodioxane (1) as a function of temperature (pressure: 1550 psig; reaction time: 1 hr; catalyst: sulfided Co-Mo/Al₂O₃).

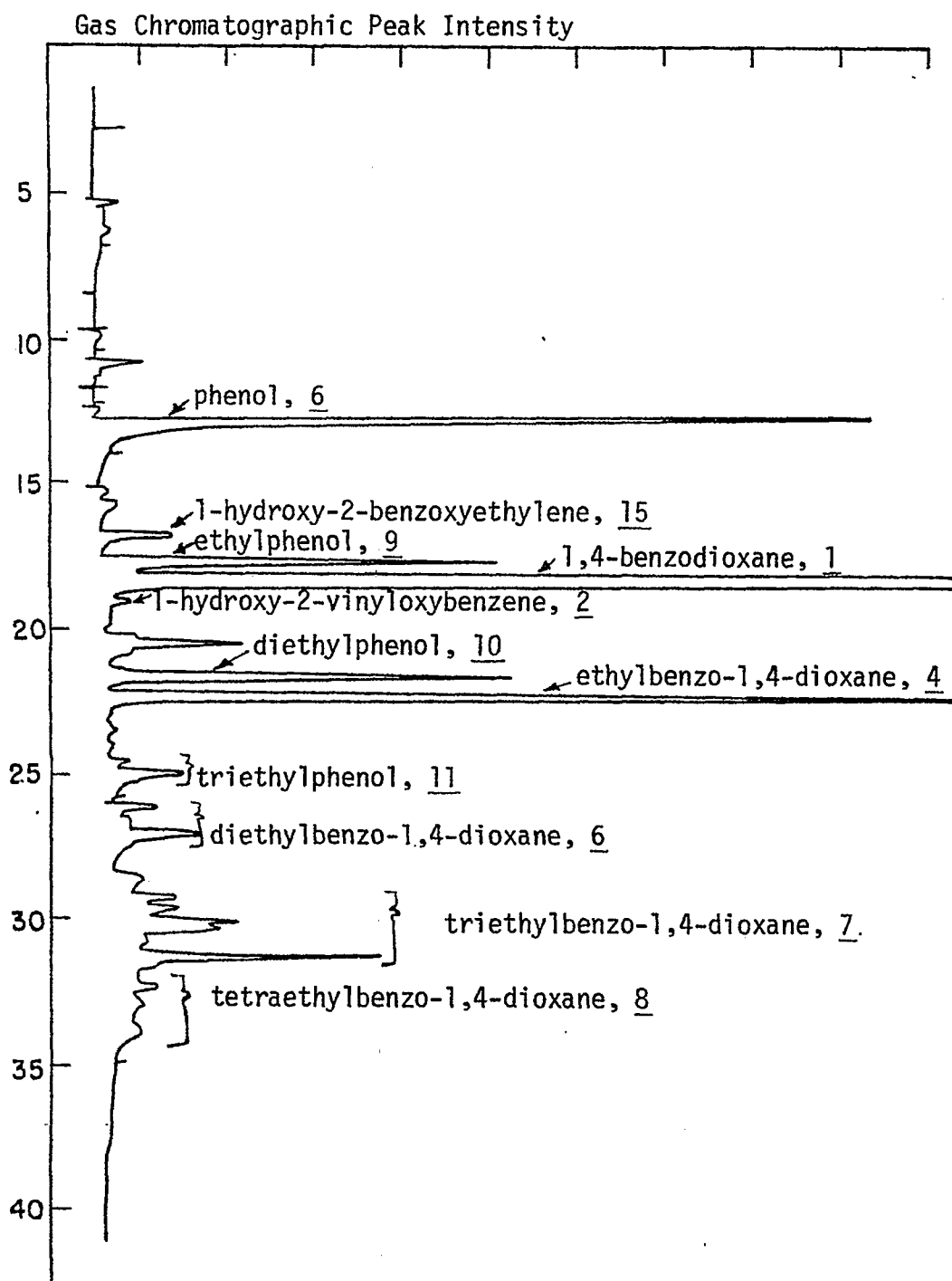


Figure 5. Typical gas chromatogram of liquid products from hydrodeoxygenation of 1,4-benzodioxane (1). Column 10' x 1/8" OD tube packed with 6% Dexsil 300 on 100-120 mesh chromosorb W-AW; F1 detector; flow rate (cc/min): helium, 45; hydrogen, 70; air, 285; initial temperature, 300C, heating rate 80C/min; final temperature, 2700C.

Task 7

Denitrogenation and Deoxygenation of CD Liquids and Related N- and O- Compounds

Faculty Advisor: J. Shabtai
C. Russell
Graduate Student: J. Peterson

Introduction

The main objective of this research project is to develop effective catalyst systems and processing conditions for reductive hydrodenitrogenation (HDN), as well as for direct (non-reductive) denitrogenation, of coal-derived liquids (CDL) in a wide range of nitrogen contents and structural type composition. This is of particular importance in view of the higher concentration of nitrogen-containing compounds in CDL as compared to that of petroleum feedstocks. For a better understanding of denitrogenation processes, the project includes systematic denitrogenation studies not only of CDL but also of related model N-containing compounds found in such liquids as phenanthridine, 1,10-phenanthroline, carbazoles, acridines, etc., as a function of catalyst type and experimental variables. A part of the study is concerned with determination of the rate, mechanism and stereochemistry of HDN of structurally distinct N-containing aromatic systems in the presence of sulfided catalysts.

Project Status

The present report discusses some initial results obtained in a study of the hydrogenation reactions of phenanthridine (1) over a sulfided Ni-W/Al₂O₃ catalyst. Hydrogenation reactions were carried out in an autoclave system described elsewhere.¹ Reaction products were identified by a combination of gas chromatography, mass spectrometry and by comparison with pure reference compounds.

Changes in product composition from hydrogenation of 1 were first investigated as a function of reaction temperature in the range of 300-380°C using a constant pressure of 2500 psig. Results obtained are given in Table I. An example of a gas chromatographic separation of products from 1 is given in Figure I.

As seen in Table I, the main products from 1 observed at 300°C are 1,2,3,4,5,6,13,14-octahydrophenanthridine (2) and 5,6,7,8,9,10,11,12-octahydrophenanthridine (3). Small amounts of 1,2,3,4-tetrahydrophenanthrine (4) and 7,8,9,10-tetrahydrophenanthrine (5), which are anticipated primary products in a stepwise hydrogenation of 1, are also found at this temperature. The other expected primary product, 5,6-dihydrophenanthridine (6), is not observed at 300°C possibly because of fast secondary reactions (studies below 300°C are presently underway to determine whether this compound is an important first step intermediate in the hydrogenation reaction). Considerable amounts of the completely

hydrogenated product, perhydrophenanthridine (7) are also formed. With an increase in temperature between 300-350°C, the concentration of 2, 3 and 7 gradually decreases while that of the anticipated HDN products, methylsubstituted biphenyl derivatives (8), gradually increases. In the range of 350-380°C such bicyclic products (8) are gradually converted into monocyclic derivatives (C₆-C₈ benzenes and cyclohexanes) by hydrogenolysis of the C-C bond bridging the two rings in 8.

These results suggest that in the temperature range studied so far at least two rings must be saturated before removal of nitrogen from the middle ring. The accumulation of the octahydro-derivatives 2 and 3, and the perhydro-derivative 7, which is observed before the appearance of the denitrogenated bicyclic product 8, supports this conclusion. Also a rather high hydrogen consumption is involved in the removal of each middle-ring nitrogen. However, the HDN reaction of phenanthridine (1) is fundamentally different from that of other tricyclic N-containing compounds, e.g., 5,6- and 7,8-benzoquinolines, leading finally to monocyclic rather than bicyclic HDN products.

The products obtained from HDN of 1 can be rationalized by a mechanism suggested in Figure 2.

Future Work

The HDN reactions of phenanthridine will be studied at reaction temperatures between 200-300°C to clarify the nature of the early hydrogenation steps in the process. An autoclave modified for determination of kinetic rate constants will then be used to verify the mechanism of Figure 2. This autoclave will also be used to verify proposed reaction networks for 5,6-benzoquinoline and 7,8-benzoquinoline.¹

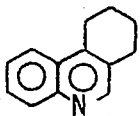
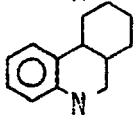
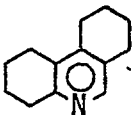
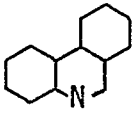
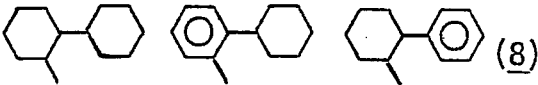
Work will be initiated on nonreductive denitrogenation of CDL and related model compounds via nitride formation.

Reference

1. L. Veluswamy, Ph.D. Thesis, University of Utah, Salt Lake City, Utah, 1977.

TABLE 1

CHANGE IN PRODUCT COMPOSITION FROM HYDRODENITROGENATION
OF PHENANTHRIDINE AS A FUNCTION OF TEMPERATURE AT
2500 PSIG, (CATALYST: SULFIDED Ni-W/Al₂O₃)^a

TEMPERATURE, °C	300	350	380
CONVERSION, MOLE %	100	100	100
PRODUCT COMPONENTS, MOLE %:			
 (4), (5)	3.55	3.18	2.94
 (2), (3)	66.34	49.36	18.03
 (6)	---	4.59	5.69
 (7)	27.19	15.82	14.54
 (8)	2.92	21.84	36.68
XYLENES	---	---	9.67
TOLUENE	---	0.38	2.12
METHYLCYCLOHEXANE	---	1.18	3.34
BENZENE	---	1.68	5.71
CYCLOHEXANE	---	1.97	1.26

^aIn each experiment 10g of 1 and 1 g of sphericat 550 catalyst (Ni-W/Al₂O₃) were used with a reaction time of 3 hr.

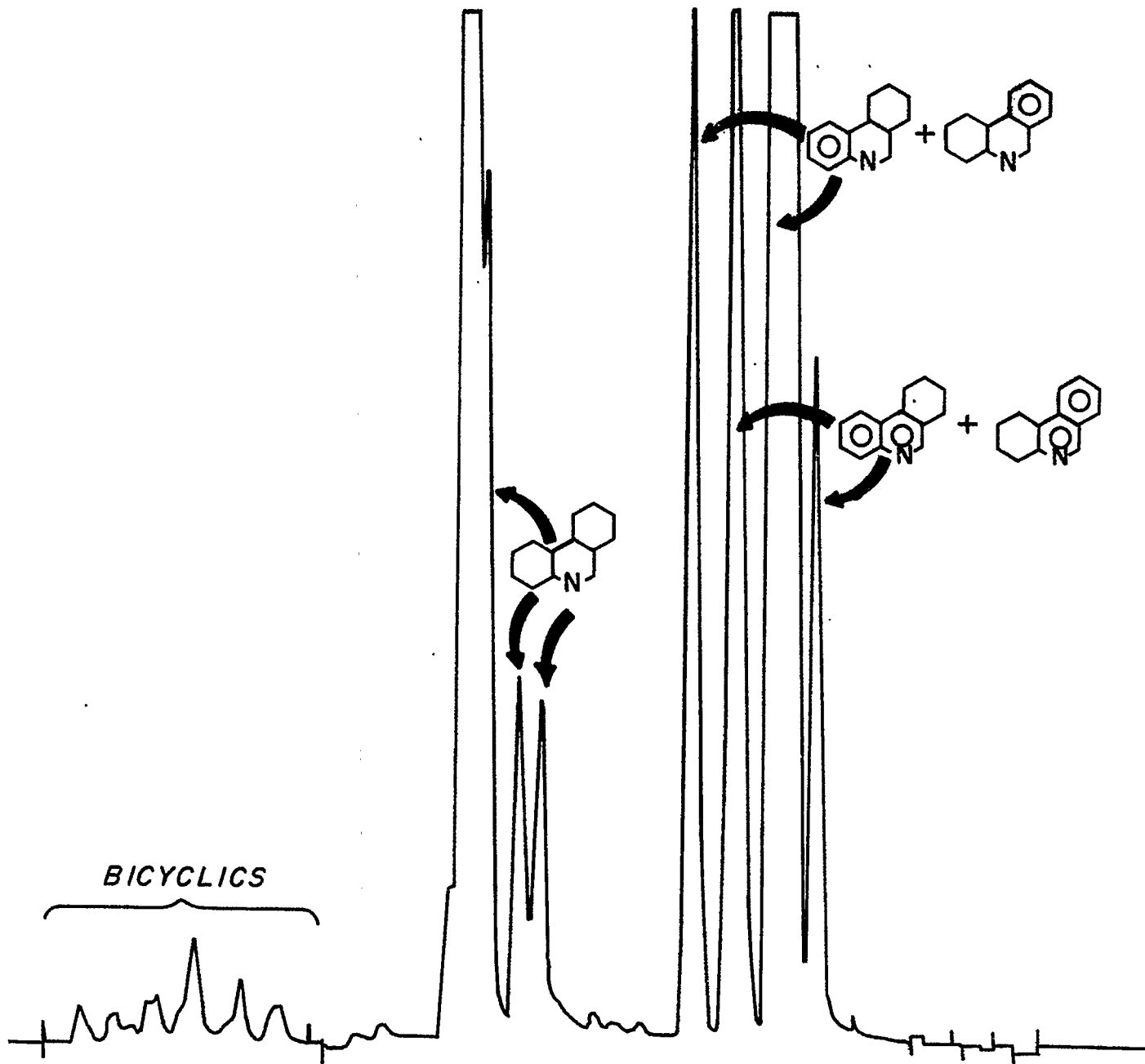


Figure 1. A typical gas chromatographic separation of products of hydrogenation of phenanthridine. (Column: 10' x 1/8"; 6% Dexil 300 on Chromosorb; Program: 60 - 270°C at 40°C/min.)

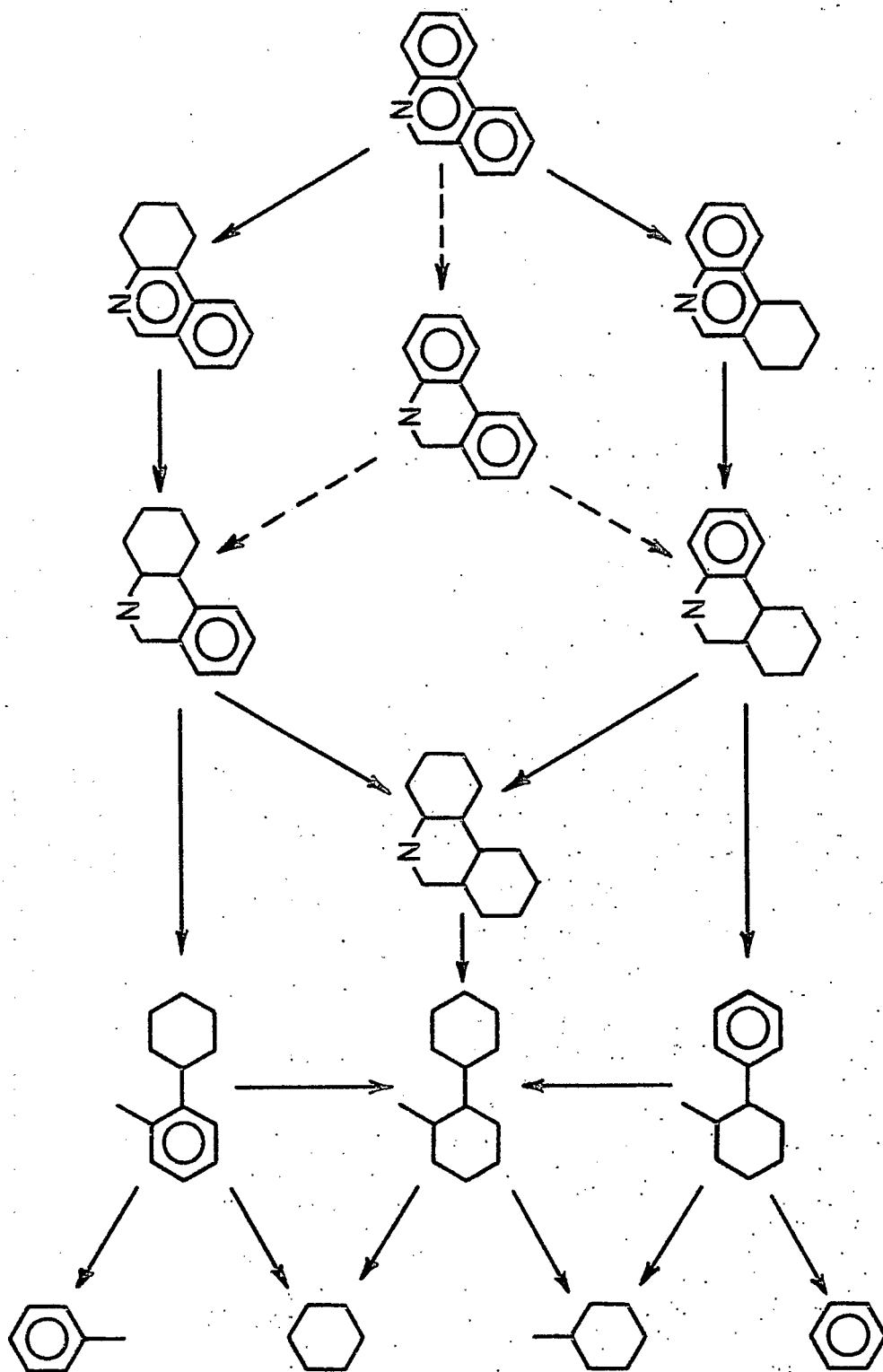


Figure 2. Indicated mechanism for phenanthridine hydrodenitrogenation over a sulfided Ni-W/Al₂O₃ catalyst.

Task 8

Catalytic Cracking of Hydrogenated Coal-Derived Liquids and Related Compounds

Faculty Advisors: J. Shabtai
A.G. Oblad
Graduate Student: S. Sunder

Introduction

Hydrogenation followed by catalytic cracking provides a feasible process sequence for conversion of coal liquids into conventional fuels. Such a sequence has certain advantages in comparison with a hydrocracking-catalytic reforming scheme.¹

The present project is concerned with the following interrelated subjects: (1) systematic catalytic cracking studies of model polycyclic naphthenes and naphthenoaromatics found in hydrogenated coal liquids, e.g., decalin, perhydrophenanthrene, tetralin, 1,2,3,4,5,6,7,8-octahydroanthracene, and 9,10-dihydrophenanthrene, as a function of catalyst type and operating conditions, and (2) systematic catalytic cracking studies of hydro-treated middle-heavy distillate from SRC II as a function of the same variables.

Project Status

Results from catalytic cracking studies of model polycyclic naphthenes, e.g., decalin and perhydrophenanthrene, were reported earlier. Results from systematic catalytic cracking studies of model polycyclic naphthenoaromatics, e.g., tetralin, 1,2,3,4,5,6,7,8-octahydroanthracene, 9,10-dihydrophenanthrene are being carried out. Results obtained with tetralin (18) as a feedstock are summarized in this report.

Catalytic cracking of tetralin (18) was investigated as a function of reaction temperature and LHSV, using the same apparatus and catalyst (Mobil Durabead-8) as in the study of decalin (1). The total process time in each experiment was kept constant at 30 min.

Table 1 and Figures 1-3 summarize the change in product composition from catalytic cracking of 18 as a function of reaction temperature (350-500°C) keeping a constant LHSV=0.60 hr⁻¹. As seen from Table 1 and Fig 1, the conversion of 18 increases gradually with an increase in temperature (from 11% at 350°C to 96% at 500°C). The selectivity for liquid formation is high for the entire temperature range studied. The liquid yield is higher than 87% between 400°C and 475°C, passing through a maximum (91%) at ca. 450°C. Below 400°C the liquid yield is somewhat lower due to considerable coke formation. However, at higher temperatures (450-500°C), the liquid yield is reduced due to an increase in secondary cracking reactions. Coke formation, which is ca. 24% at 350°C, steadily decreases until it is only ca. 3% at 500°C. Gas products, however, increase from about 1% at 350°C to 14% at 500°C. Figure 2 shows that the gaseous products consist mainly of saturated C₃ and C₄ hydrocarbons.

As seen from Table 1 and Figure 3, naphthalene (19), apparently formed by hydrogen transfer, is the major product between 350^o and 500^oC, but it gradually decreases in concentration above 450^oC. Methyl naphthalenes (20a) and C₁₂-alkyl naphthalenes (21a) are also formed (6 to 10 mol/100 mol of 18 converted). The anticipated primary cracking products from tetralin (18), i.e., C₁₀-alkenyl benzenes (24, 25) (plotted in Figure 3 as free and condensed as coke) decrease steadily from ca. 20% at 350^oC to ca. 5% at 525^oC. The C₁₀-alkyl benzenes (15, 16), derived by saturation of the side chains of the C₁₀-alkenyl benzenes (24, 25), go through an early maximum at ca. 375^oC and then decrease due to dealkylation at higher temperatures. The C₆-C₉ benzenes (12, 13, 14) formed by partial or complete dealkylation of such C₁₀-benzenes (15, 16, 24, 25) gradually increase with increasing temperature and are indicated as the main products above 525^oC. Decalin (1), apparently formed by hydrogen transfer reactions of 18, is found in only small amounts (8 mol/100 moles of 18 reacted) at 350^oC and decreases gradually due to cracking reactions at higher temperatures, yielding C₆-C₇ cyclanes (7, 8) and C₅-C₆ open-chain products (2, 3, 4, 5). The C₆-C₇ cyclanes go through a maximum at ca. 475^oC and then decrease due to secondary cracking reactions. The C₅-C₆ paraffins and olefins increase steadily with increasing temperature to about 5.5 mol/100 mol of 18 cracked at 500^oC.

Table 2 and Figures 4-6 summarize the change in product composition from catalytic cracking of 18 as a function of LHSV (0.16-9.78 hr⁻¹) at a constant reaction temperature of 425^oC. The changes in product distribution follow similar patterns as in the study of the temperature effect (Table 1, Figures 1-3).

An appropriate reaction mechanism has been developed to describe the change in product composition with the reaction variables studied.

The following conclusion can be reached on the basis of the results obtained. Tetralin (18) undergoes smooth catalytic cracking in the entire temperature range studied. However coke formation is high at low temperatures (350-400^oC), and formation of bicyclic liquid components, e.g., naphthalene and alkyl naphthalenes is high at intermediate temperatures (400-500^oC). Thus high temperatures (> 550^oC) are required to obtain desirable products such as benzene derivatives and C₅-C₆ open-chain products from tetralin (18).

Future Work

Systematic catalytic cracking studies on 1,2,3,4,5,6,7,8-octahydroanthracene, 9,10-dihydrophenanthrene and hydrogenated SRC II are being continued.

Reference

1. L. R. Veluswamy, Ph.D. Thesis, University of Utah, Salt Lake City, Utah 1977.

Table 1
 Change in Product Composition from Cracking of Tetralin(18)

as a Function of Reaction Temperature^{a-d}.

Experiment Number	THN 05	THN 09	THN 04	THN 08	THN 06	THN 07	THN 10
Reaction Temperature, °C	350	375	400	425	450	475	500
Conversion, % by wt. of feed (18)	10.81	16.65	29.20	50.55	70.33	88.46	95.66
Yield, % by wt. of reacted 18							
Gases	0.83	2.33	3.29	4.97	5.17	8.82	14.32
Liquids	75.23	84.58	87.91	89.41	91.26	87.91	82.73
Coke	23.68	13.00	8.76	5.78	3.57	3.27	2.92
Product Distribution, mol./100 mol. of reacted 18							
H ₂	-	-	-	-	0.17	0.66	1.42
CH ₄	-	-	0.07	0.08	0.17	0.41	1.07
C ₂ H ₆	-	-	0.04	0.09	0.18	0.44	0.97

Table 2

Change in Product Composition from Cracking of Tetralin(18)

as a Function of LHSV^{a-d}.

Experiment Number	THN 15	THN 12	THN 11	THN 08	THN 13	THN 14
LHSV, hr ⁻¹	9.78	2.95	1.02	0.57	0.29	0.16
Conversion, % by wt. of feed <u>18</u>	5.20	13.93	30.26	50.55	63.07	71.62
Yield, % by wt. of reacted <u>18</u>						
Gases	3.09	2.75	3.50	4.97	6.96	7.43
Liquids	86.16	91.30	91.31	89.41	87.72	86.91
Coke	10.74	5.95	5.24	5.78	5.31	5.65
Product Distribution, mol./100 mol. of reacted <u>18</u>						
H ₂	-	0.12	0.48	0.05	0.13	0.40
CH ₄	0.16	0.07	0.06	0.08	0.11	0.14
C ₂ H ₆	0.04	0.04	0.05	0.09	0.14	0.17

Table 2 - Continued

	LHSV, hr ⁻¹							
	9.78	2.95	1.02	0.57	0.29	0.16		
C ₂ H ₄	-	-	0.05	-	-	0.19		
C ₃ H ₈	2.76	2.83	3.68	4.89	6.70	8.39		
i-C ₄ H ₁₀	2.44	2.47	3.19	4.93	6.46	7.20		
n-C ₄ H ₁₀	1.66	1.59	1.91	2.60	3.14	3.59		
Butenes	-	-	-	-	-	-		
C ₅ - C ₆ (<u>2,3,4,5</u>)	1.40	0.78	1.42	2.50	3.32	3.38		
Methylcyclopentane (<u>7</u>)	1.11	0.50	2.16	2.99	3.17	3.29		
Dimethylcyclopentane (<u>8a</u>) + 	0.34	0.90	1.06	1.09	1.62	1.58		
Methylcyclohexane (<u>8b</u>) 								
Benzene (<u>12</u>)	8.21	9.69	10.80	11.47	10.51	11.24		
Toluene (<u>13</u>)	0.57	1.46	2.15	2.98	3.57	3.64		
Ethylbenzene (<u>14a</u>) + Xylenes (<u>14b</u>)	0.43	2.17	2.68	2.35	2.83	2.96		
C ₉ -alkylbenzenes (<u>14c</u>)	1.03	2.18	2.49	3.04	3.23	3.11		

Table 2 - Continued

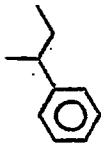
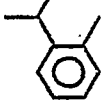
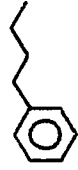
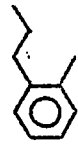
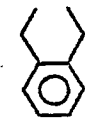
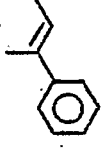
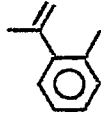
LHSV, hr ⁻¹		9.78	2.95	1.02	0.57	0.29	0.16
i,C ₁₀ -alkyl...		0.56	0.78	0.74	0.66	1.01	0.98
	<u>15a</u>						
benzenes (15)		6.20	5.70	5.55	4.49	3.91	3.95
	<u>15b</u>						
n,C ₁₀ -alkyl...		4.08	4.22	4.05	3.54	3.20	3.14
	<u>16a</u>						
							
benzenes (16)		9.78	2.95	1.02	0.57	0.29	0.16
	<u>16b</u>						
i,C ₁₀ -alkenyl...		0.56	0.78	0.74	0.66	1.01	0.98
	<u>24a</u>						
benzenes (24)		6.20	5.70	5.55	4.49	3.91	3.95
	<u>24b</u>						

Table 2 - Continued


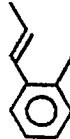
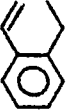
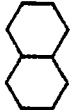

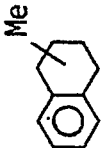
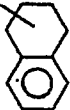

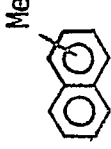
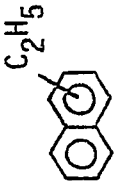
	LHSV, hr ⁻¹	9.78	2.95	1.02	0.57	0.29	0.16
n,C ₁₀ -alkenyl...	 <u>,25a</u>						
benzenes(<u>25</u>)	 <u>,25b</u>	6.35	7.63	7.80	7.65	6.68	6.67
	 <u>,25c</u>						
Decalin(<u>1</u>),		10.42	5.01	3.21	2.18	1.51	1.31
Methylindans(<u>17</u>),	 Me	-	-	0.79	1.35	1.38	1.44
	 Me						
Methyltetralins(<u>20b</u>),		2.36	3.23	2.94	1.63	1.79	1.44
Naphthalene(<u>19</u>),		46.40	48.84	45.07	44.07	43.03	40.90

Table 2 - Continued

LHSV, hr ⁻¹	9.78	2.95	1.02	0.57	0.29	0.16
Methylnaphthalenes (20a), 	1.03	1.24	1.09	3.19	3.69	4.38
C ₁₂ -alkylnaphthalenes (21a), 	0.97	2.40	3.01	2.59	3.17	3.19

(a) In each experiment 6.8 g of 18 was used;

(b) Catalyst, Durabead-8;

(c) Run time, 30 min.;

(d) Reaction temperature, 425°C.

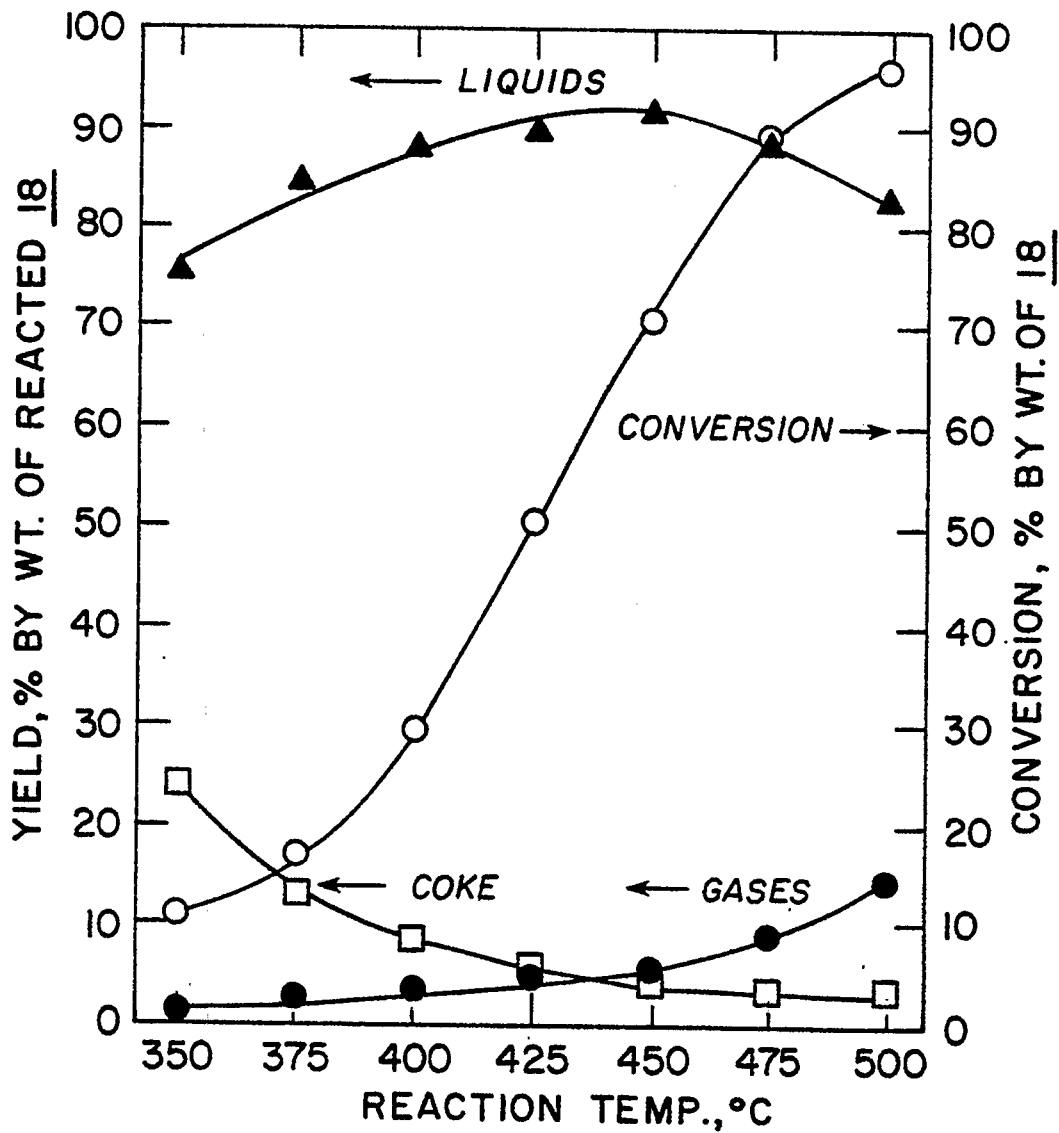


Figure 1. Distribution of Coke, Liquid and Gaseous Products from Cracking of Tetralin(18), as a Function of Reaction Temperature (catalyst, Durabead-8; LHSV, 0.60 hr^{-1}).

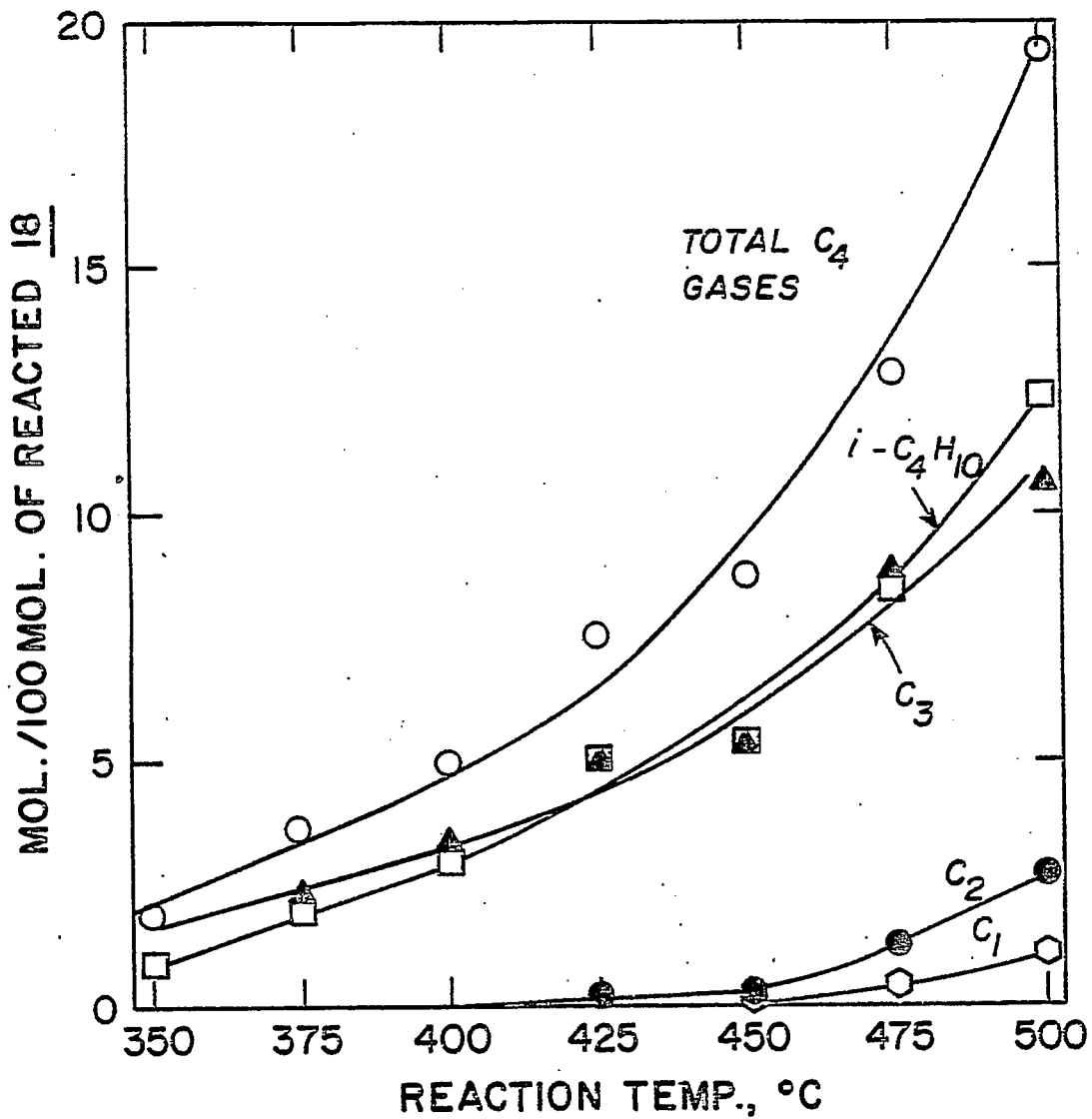


Figure 2. Change in Gaseous Product Composition from Cracking of Tetralin(18), as a Function of Reaction Temperature (catalyst, Durabead-8; LHSV, 0.60 hr^{-1}).

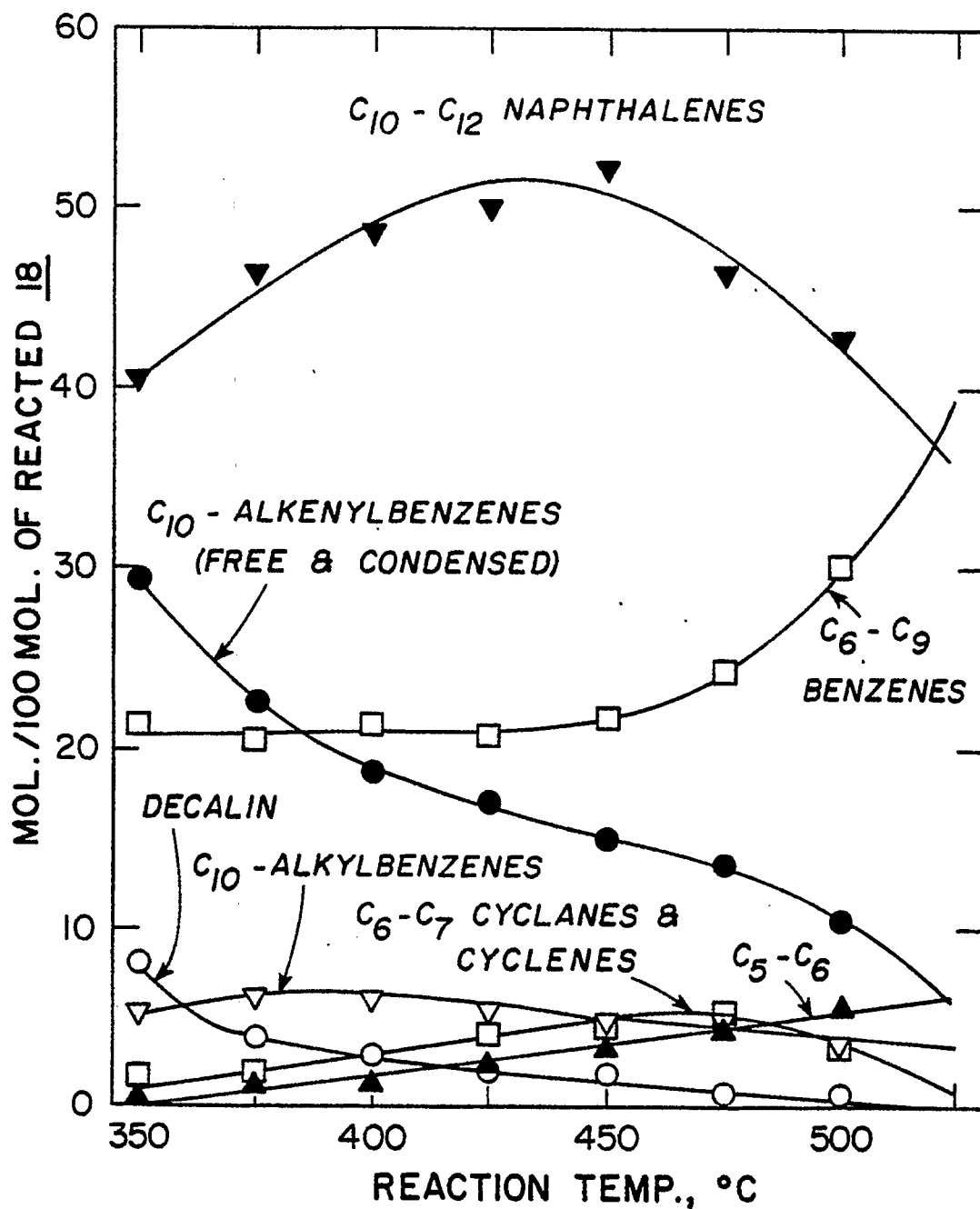


Figure 3 . Change in Liquid Product Composition from Cracking of Tetralin(18), as a Function of Reaction Temperature (catalyst, Durabead-8; LHSV, 0.60 hr⁻¹).

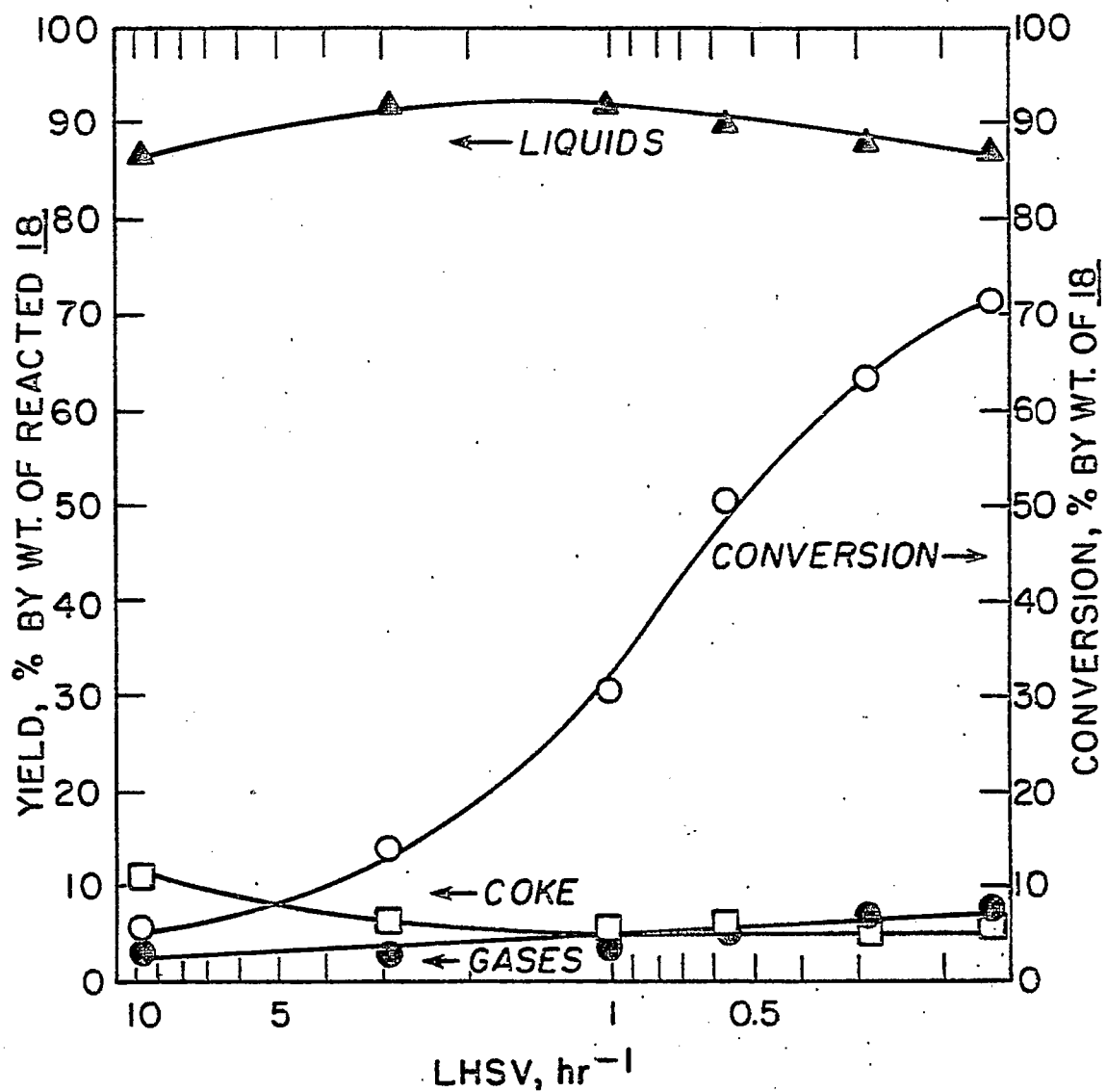


Figure 4. Distribution of Coke, Liquid and Gaseous Products from Cracking of Tetralin(18), as a Function of LHSV (catalyst, Durabead-8; reaction temperature, 425^oC).

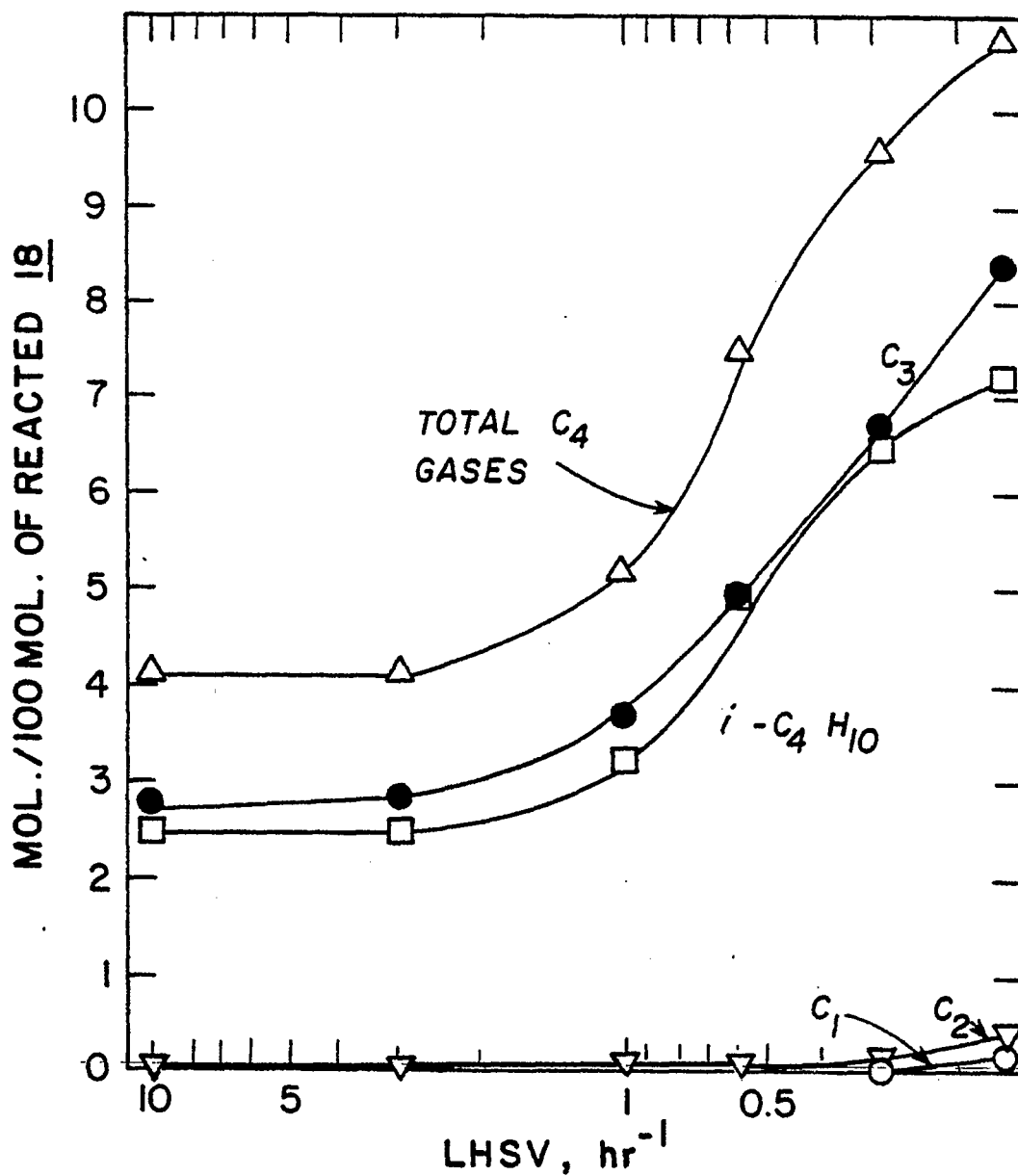


Figure 5. Change in Gaseous Product Composition from Cracking of Tetralin(18) as a Function of LHSV (catalyst, Durabead-8; reaction temperature, 425°C).

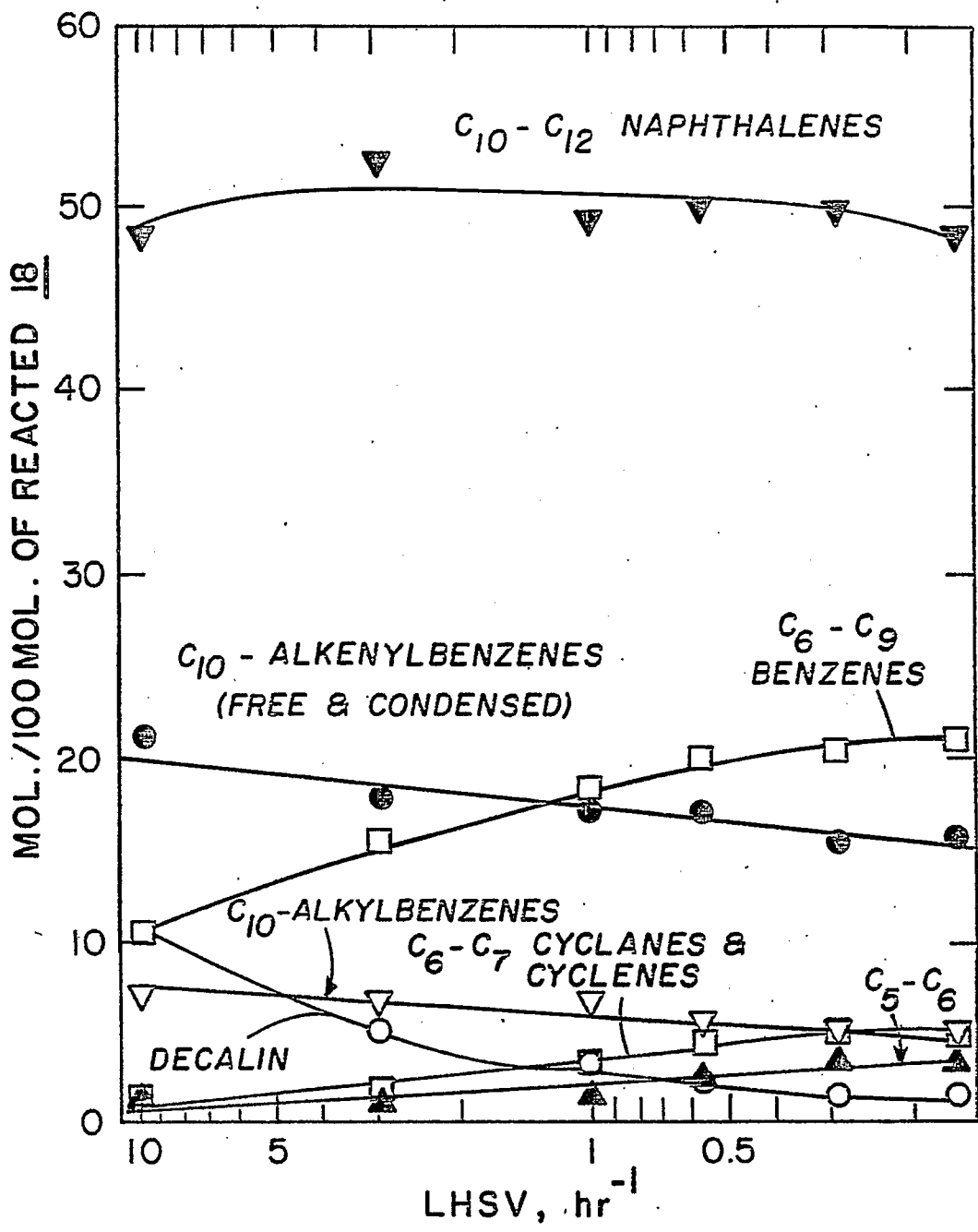


Figure 6 . Change in Liquid Product Composition from Cracking of Tetralin(18) as a Function of LHSV (catalyst, Durabead-8; reaction temperature, 425°C).

Task 11

The Effects of Poisoning on the Desulfurization Activity of Cobalt-Molybdate Catalysts

Faculty Advisor: F.E. Massoth
Graduate Student: R. Ramachandran

Introduction

The importance of cobalt-molybdena catalysts for hydrotreating and hydrodesulfurization of petroleum feed stocks is well-known. These catalysts are also being studied for hydrodesulfurization and liquefaction of coal slurries and coal-derived liquids. However, these complex feed stocks result in rapid deactivation of the catalysts. To gain an insight into the deactivation mechanism, detailed kinetics of the hydrodesulfurization of the model compound benzothiophene are compared before and after addition of various poisons and coke precursors. The studies are planned using a constant stirred microbalance reactor, which enables simultaneous measurement of catalyst weight change and activity.

Initial tests with the flow microbalance reactor showed that perfect gas mixing was not achieved when injecting a liquid feed (gaseous at reaction temperature) directly into the reactor. Modifications incorporated into a new reactor design have eliminated the problem and improved the mechanical stability of the system.

Preliminary tests of benzothiophene hydrodesulfurization over a sulfided CoMo/Al₂O₃ catalyst showed the rate to be proportional to benzothiophene and hydrogen and inhibited by benzothiophene and H₂S. Pyridine and quinoline were poisons for the reaction. Advantage of this finding was taken to develop a technique for assaying active catalyst sites by successive poisoning-activity measurements.

Adsorption of H₂S on the sulfided catalyst was reversible and correlated with a Langmuir adsorption isotherm. Chemisorption of pyridine lowered H₂S adsorption, indicating a competition for adsorption sites.

Temperature-programmed desorption studies of thiophene on the CoMo/Al₂O₃ catalyst showed a complex desorption pattern when using a thermal conductivity detector to monitor the effluent gas stream. Employing a mass spectrometer to analyze the off gases, appreciable amounts of butene and H₂S were found, as well as desorbed thiophene, signifying partial decomposition of the thiophene during temperature-programmed desorption. Similar patterns were observed on aged and poisoned catalyst, with less overall adsorption of thiophene in the latter two cases.

Project Status

Benzothiophene (BT) hydrodesulfurization (HDS) kinetics were undertaken on a commercial Ketjen 3% Co 8% Mo/Al₂O₃ catalyst using the constant stirred microbalance reactor. The apparatus was identical to that described previously,¹ except for the modified reactor design.² Preliminary

experiments were carried out varying catalyst particle size and stirrer speed to establish a regime without mass transfer influence. The catalyst (150 mg) was sulfided using 10% H₂S in H₂ at 400°C for 2 hours, flushed in He at 400°C for 1 hour before cooling to the reaction temperature of 350°C. A minimum H₂S flow over the catalyst was maintained during the series of experiments to avoid any catalyst structural changes.³ The BT, dissolved in n-heptane solvent, was pumped through the reactor in a H₂-H₂S flow mixture chosen as the standard condition. The extent of the BT reaction was analyzed by gas chromatography using an FID detector and a 6 foot column of 3% SE-30. Ethyl benzene was the only hydrocarbon product observed under the present reaction conditions. The BT was fed continuously under the standard flow conditions until the catalyst weight reached a fairly steady condition, as observed by constancy in catalyst weight and conversion. About 2 weeks were required for the catalyst to reach this state. Subsequently, 4-6 hours were needed to reach a new steady state after each change in reaction conditions.

Figure 1 shows the catalyst weight changes which occurred during the kinetic series. Although the catalyst continued to gain weight over the time period involved, these changes were relatively smaller than the large weight obtained during the initial exposure of the sulfided catalyst to BT. During the period of the kinetic series, catalyst conversions under the standard condition remained essentially constant, indicating that the small additional weight increases did not affect the catalyst activity. Weight changes at various reaction conditions were essentially reversible and are related to different amounts of adsorbed species present on the catalyst.

The kinetic series was carried out by systematic variation of the partial pressures of BT, H₂S, H₂ and He. Table 1 gives the partial pressures and rate data for this series. Massoth⁴ and others⁵ have shown that the HDS reaction rate follows a Langmuir-Hinshelwood form. Table 2 shows the different types of rate equations tried for fitting the data. The University of Utah Computer Center ZXSSQ subroutine, based on the Levenberg-Marquardt algorithm, was used to fit the data to the different rate equations. This program gives the rate constants, adsorption equilibrium constants and the sum of squares between the observed and the calculated rates. Table 2 indicates that it is rather difficult to differentiate between rate equations, especially for the cases 2, 4 and 6, just based on the sum of squares. But some interesting conclusions can be reached from the correlations: (1) BT and H₂S compete for the same type of site and they inhibit the reaction; (2) H₂ adsorbs on a different site and it also inhibits the reaction; (3) BT adsorbs much stronger than H₂S and (4) the presence of a square in the H₂S-BT term improves the sum of squares considerably, indicating a possible two site adsorption as initially reported by Satterfield.⁶ From these data it is difficult to say whether H₂ adsorbs on the catalyst associatively or dissociatively.

Temperature-programmed desorption (TPD) experiments were also continued during this period using H₂S as the adsorbate. The experimental set up is the same as described earlier.⁷ The experimental sequence consisted of: (1) sulfide the catalyst using 10% H₂S in H₂ at 400°C for 2 hours, (2) flush in He at 400°C for 1 hour, (3) cool to 100°C in He, (4) TPD in He to 350°C, (5) cool to 100°C in He, (6) TPD in H₂ to 350°C, (7) cool in He to 100°C, (8) adsorb H₂S/H₂ at 100°C for 1/2 hour, (9) desorb in He for 1 hour at 100°C, (10) TPD in He to 350°C, (11) cool to 100°C in He, (12) TPD in He

to 350°C, (13) cool in He to 100°C and (14) TPD in H₂ to 350°C.

Figure 2 shows the above sequence of experiments for 8% Mo/γ-Al₂O₃ and γ-Al₂O₃. Curve 1 shows that during Step 6, H₂S desorbs from the catalyst even though the catalyst was previously stripped in He at 400°C. But in the case of γ-Al₂O₃, no H₂S was observed, indicating that the S removed as H₂S in the catalyst is associated with the Mo phase. During Step 10, both Mo/Al₂O₃ and Al₂O₃ desorbed H₂S (curve 2), but Mo/Al₂O₃ also desorbed some H₂ whereas alumina did not. Also, during Step 14, (curve 3) H₂S desorption was observed with the catalyst whereas no H₂S was observed with Al₂O₃. These results indicate that part of the H₂S adsorbs dissociatively on the catalyst. Also the Mo/Al₂O₃ does not seem to possess any alumina character for H₂S adsorption.

Additional H₂S desorption studies were done on aged and poisoned Mo/Al₂O₃ catalyst. In the former case, the presulfided catalyst was exposed to a thiophene-H₂ reaction mixture for an overnight period at 350°C. In the latter case, the aged catalyst was subsequently exposed to quinoline for one hour, also at 350°C. A subsequent one-hour He flush post-treatment at 350°C was applied in both cases. Figure 3 compares the results for fresh sulfided, aged and poisoned catalysts. In these runs, TPD in He was followed by TPD in H₂ after adsorbing H₂S at 100°C. The desorption curves in He are due to reversibly adsorbed H₂S, whereas those in H₂ are due to sulfur left from dissociative adsorption of the H₂S. The amount of H₂S adsorbed on the aged and poisoned catalyst was considerably less than on the fresh sulfided catalyst, although the desorption patterns were similar in nature for all cases. It therefore appears that the nature of the adsorption sites for H₂S has not changed on the aged and poisoned catalyst, only their number has decreased.

Future Work

A kinetic series of experiments will be carried out on hexene hydrogenation and on a mixed feed of BT-hexene. This will be followed by poisoning experiments using quinoline. The TPD experiments will be continued using thiophene as the adsorbate.

References

1. W.H. Wiser et al., DOE Contract No. E(49-18)-2006, Quarterly Progress Report, Salt Lake City, Utah, Jan-Mar 1976.
2. ibid., April-June 1977.
3. C.H. Broderick, G.C.A. Schuit and B.C. Gates, J. Catalysis, 54, 94 (1978).
4. F.E. Massoth, J. Catalysis, 47, 316 (1977).
5. O. Weisser and S. Landa, "Sulfide Catalysts, Their Properties and Applications," Pergamon, New York, N.Y., 1973.
6. C.N. Satterfield and G.W. Roberts, AIChE J., 14, 159 (1968).
7. W.H. Wiser et al., DOE Contract No. E(49-18)-2006, Quarterly Progress Report, Salt Lake City, Utah Apr-Jun 1979

Table 1. Benzothiophene Hydrodesulfurization Kinetic Data

$P_T \times 10^4$, atm	$P_S \times 10^2$, atm	P_H , atm	R_T , $\text{cm}^3/\text{min}\cdot\text{g}$
1.12	1.66	0.836	0.158
2.86	1.68	0.833	0.331
10.62	1.68	0.826	0.486
3.16	1.68	0.833	0.307
1.27	1.66	0.836	0.146
1.53	3.85	0.814	0.131
1.62	5.5	0.798	0.120
1.18	1.69	0.836	0.154
1.37	1.76	0.735	0.144
1.47	1.75	0.616	0.136
1.17	1.72	0.834	0.186
0.97	1.80	0.836	0.139
1.52	1.80	0.539	0.136
1.65	1.65	0.392	0.116
2.12	1.64	0.243	0.079
1.17	1.73	0.835	0.158
2.16	1.65	0.240	0.077

Table 2. Correlation of Data

Case #	a	b	c	d	SSOx10 ³	k _T cc/min g x 10 ³	k _T , g tm ⁻¹ 10 ³	K _S , atm ⁻¹	K _H , atm ⁻¹
<u>Dual Site*</u>									
1	1	1	1	1	3.515	4.76	5.17	52.0	0.18
2	1	2	1	1	2.987	3.17	0.98	11.2	0.18
3	2	1	1	2	3.73	44.4	5.12	52.4	2.4
4	2	2	1	2	3.134	29.4	0.98	11.3	2.4
5	1	1	0.5	2	3.505	5.22	5.17	51.8	0.018
6	1	2	0.5	2	2.984	3.46	0.98	11.2	0.017
7	1	1	0	0	3.695	4.27	5.36	53.9	--
8	1	2	0	0	3.164	2.81	1.00	11.4	--
<u>Single Site†</u>									
9	2	2	1	-	3.217	490	10.8	123.1	12.3
10	1	1	1	-	3.512	6.40	7.98	79.6	0.68

$$*R_T = \frac{k_T P_T P_H^a}{(1 + K_T P_T + K_{SPS})^b [1 + (K_{HPH})^c]^d} \quad \dagger R_T = \frac{k_T P_T P_H^a}{[1 + K_T P_T + K_{SPS} + (K_{HPH})^c]^b}$$

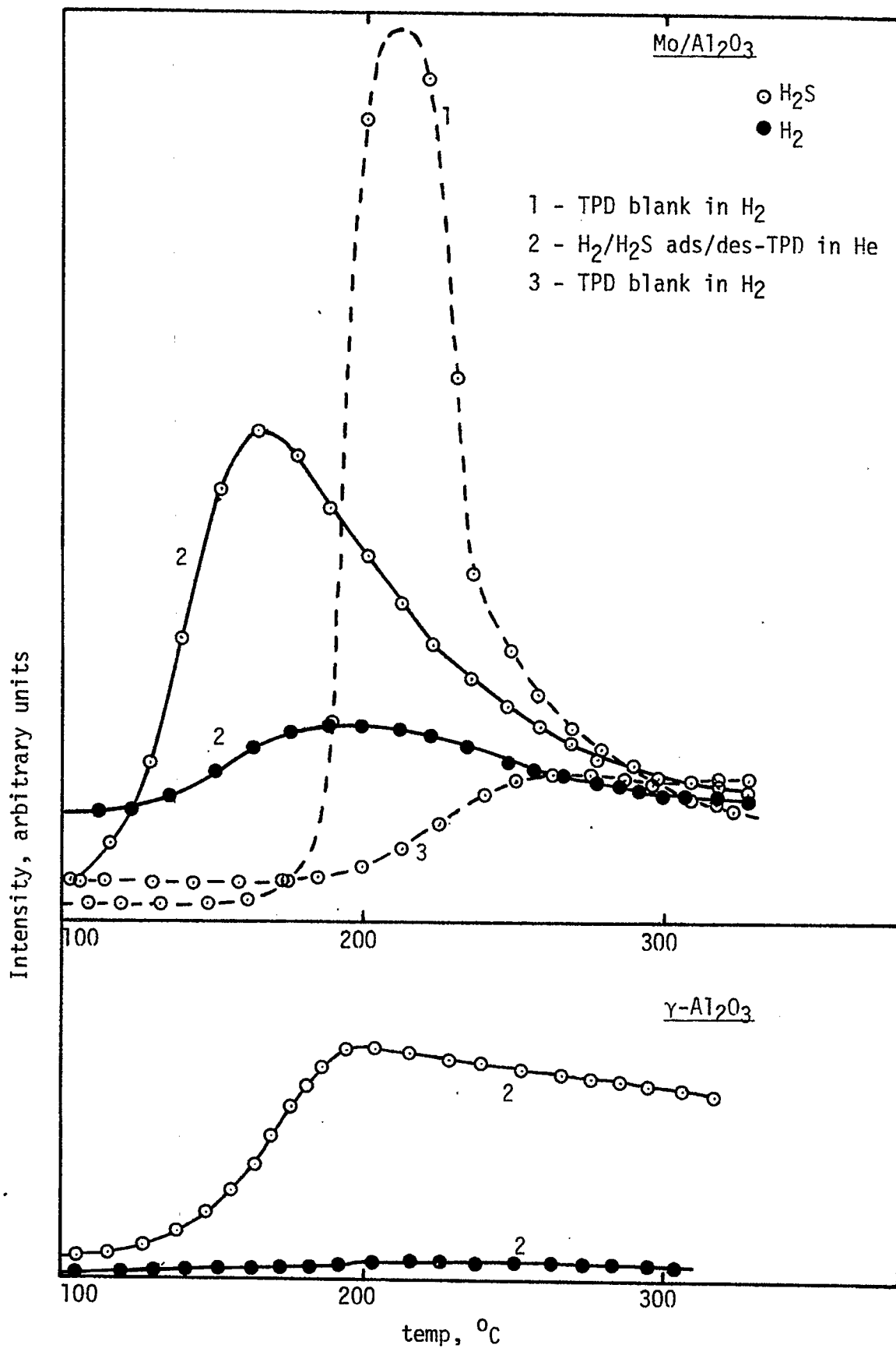


Figure 2. H₂S adsorption and TPD.

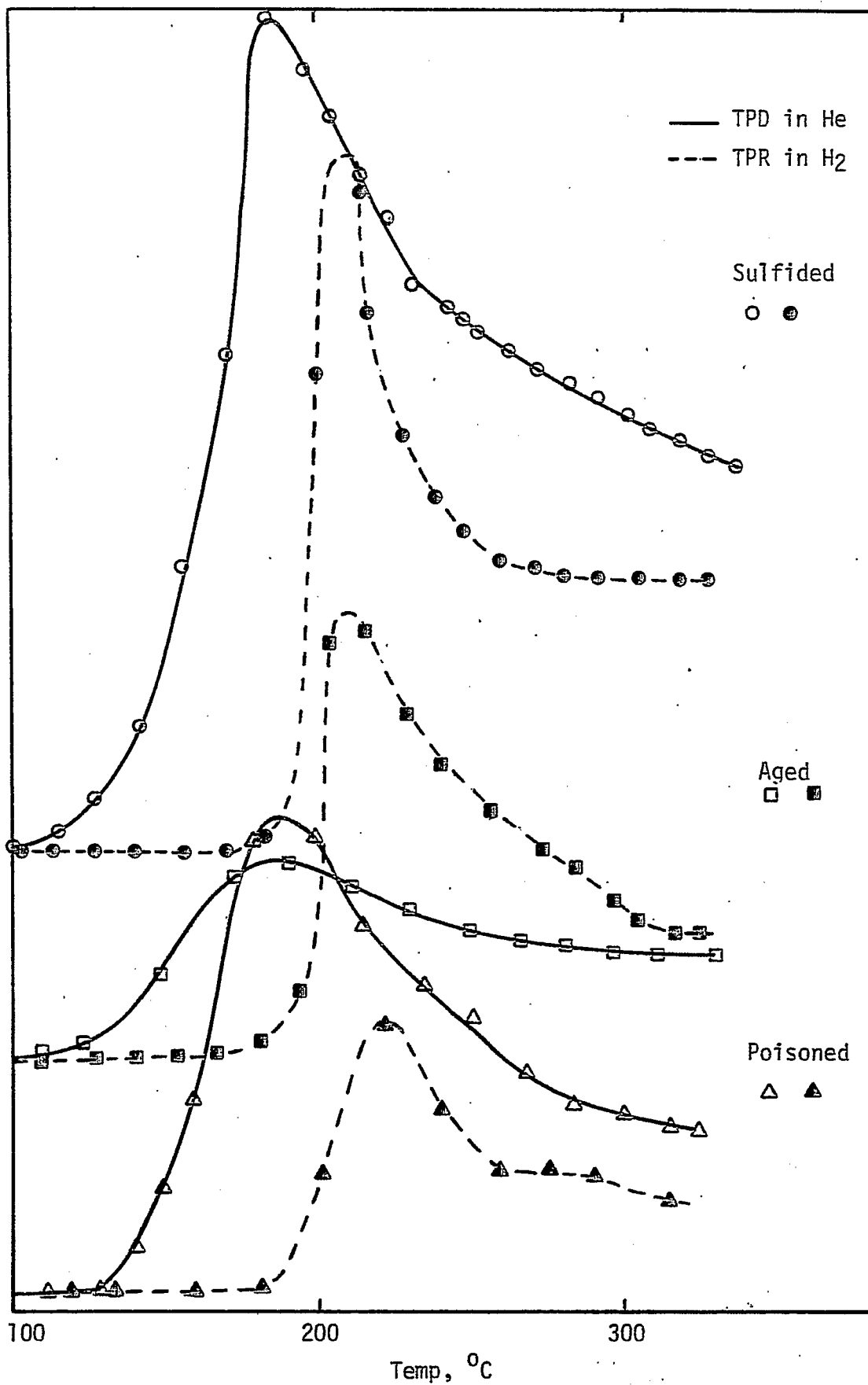


Figure 3. H₂S adsorption/ desorption on fresh, aged and poisoned catalysts.

Task 12

Diffusion of Polyaromatic Compounds in Amorphous Catalysts Supports

Faculty Advisor: F.E. Massoth

Graduate Student: A. Chantong

Introduction

This project involves assessing diffusional resistances within amorphous-type catalysts. Of primary concern is the question of whether the larger, multiring hydro-aromatics found in coal-derived liquids will have adequate accessibility to the active sites of typical processing catalysts. When molecular dimensions approach pore size diameters, the effectiveness of a particular catalyst is reduced owing to significant mass transport resistance. An extreme case occurs when molecular and pore sizes are equivalent, and pores below this size are catalytically inactive.

The project objective can be achieved through a systematic study of the effect of molecular size on sorptive diffusion rates relative to pore geometry. Conceptually, the diffusion of model aromatic compounds is carried out using a stirred batch reactor. The preferential uptake of the aromatic from the aliphatic solvent is measured using a UV spectrometer. Adsorption isotherms are determined to supplement the diffusion studies.

Initial work entailed development of a suitable reactor, measurement techniques and methods of data analysis. These demonstrated that adsorption was diffusion-controlled. Effective diffusivities were larger than predicted for pore diffusion and a surface diffusion contribution was postulated. Subsequent studies were extended to other multiaromatic compounds and aluminas with similar results. The fractional surface diffusion contribution was appreciable and about the same in all cases. Because of this, restrictive diffusion effects could not be properly evaluated. However, for the largest size compound (20 Å) and smallest average pore size alumina (50 Å) tested, a markedly lower diffusivity was obtained, indicative of a restrictive diffusion effect.

Project Status

Our early studies of diffusion of aromatic compounds in alumina catalyst supports have led us to conclude that an appreciable contribution to the diffusion flux was due to surface diffusion, which occurred simultaneously with normal pore diffusion.¹ Subsequent work with meso-tetraphenylporphyrin cast doubt on whether surface diffusion was occurring with this compound.² However, due to the large size of this compound, possible surface diffusion could be masked by restrictive diffusion, lowering the overall diffusivity. Therefore, we reinvestigated the naphthalene system to further check on surface diffusion, since its small molecular size should preclude a restrictive diffusion effect. Also, a reliable value of the bulk diffusivity needed to assess effective diffusivity data, is available for this compound.

Previous work on naphthalene gave evidence of apparent surface diffusion.^{1,3} There are two problems with this interpretation. First, the calculated tortuosity factors were lower than expected by a factor of two to three. Second, and more important, it is difficult to envision how appreciable surface diffusion can occur with the very low coverage of adsorbed naphthalene (less than 1% of alumina surface), indicating the adsorption sites are quite far apart. Since surface diffusion must occur by molecular jumps between adsorption sites, such large distances between these sites would seem to preclude this as a plausible mechanism.

New diffusion runs of naphthalene/cyclohexane with alumina catalyst L showed variable results which could be related to the catalyst sample size used. Thus, lower apparent diffusivities were obtained with larger amounts of catalysts. This indicated that bulk mass transport may be affecting the results. To eliminate this possible factor, the stirred tank reactor was modified to include baffles around the periphery of the reactor to achieve better contact between catalyst and solution. Results with the new reactor showed better consistency in that data were independent of catalyst size. Interestingly, the effective diffusivity (D_e) values were now independent of equilibrium adsorption (K), as shown in Fig 1, contrary to the earlier data. The earlier data appear to approach the new data at high values of K . This is significant because the surface diffusion should result in an increase in effectivity diffusivity with adsorption,³ which the new data do not show. Thus, the occurrence of surface diffusion becomes questionable and the previous data explicable in terms of mass transfer effects, since larger catalyst samples were used in the low K region. However, the problem of high diffusion rates remains, i.e., the average D_e is considerably higher than expected for pore diffusion, yielding an unreasonably low catalyst tortuosity factor of 0.8

Prasher and Ma report no surface diffusion occurs in alumina pellets with a 1-methylnaphthalene in cyclohexane solution.⁴ Their experiments were carried out at considerably higher solute concentrations (40,000 - 100,000 mg/l) than ours (5 - 40 mg/l). To see the effect of concentration, a diffusion run was made at a concentration of 370 mg/l. The effective diffusivity was about one-half of that obtained in the low concentration range, giving a somewhat more reasonable tortuosity factor of 1.5. A concentration effect is not generally observed in these types of diffusion studies.

A possible source of error in determining diffusivity values in adsorption-diffusion studies arises from the nature of the adsorption isotherm involved. The calculated diffusion coefficient depends on the value of the equilibrium adsorption constant, which is invariably obtained from the assumption of a linear adsorption isotherm. However, our systems are quite non-linear in this respect, as shown in Fig 2 for naphthalene with catalyst L. We had been assuming that adsorption was approximately linear in our calculations to solve the applicable differential equations in closed form. The fact that the isotherm is not linear may mean that our calculated values are in error, and may account for the unexpected concentration effect mentioned above, as well as the high diffusivities obtained. It now appears necessary to reanalyze our data employing a non-linear isotherm. This requires a numerical technique for solution.

Future Work

Isotherms will be determined for the naphthalene system at higher concentrations and additional diffusion runs will be made in this region. A

numerical technique will be developed to incorporate a non-linear isotherm into the basic differential equations for diffusion. This will be applied to the previous and new data obtained to see if this will resolve the problem of high apparent diffusivities for naphthalene. Subsequent work will involve larger aromatic molecules.

References

1. C. Kim, M.S. Thesis, University of Utah, Salt Lake City, Utah, 1978.
2. W.H. Wiser et al., DOE Contract No. E (49-18)-2006, Quarterly Progress Report, Salt Lake City, Utah, Jan - Mar 1979.
3. ibid., Oct - Dec 1978.
4. B.D. Prasher and Y.H. Ma, AIChE J., 23, 303 (1977).

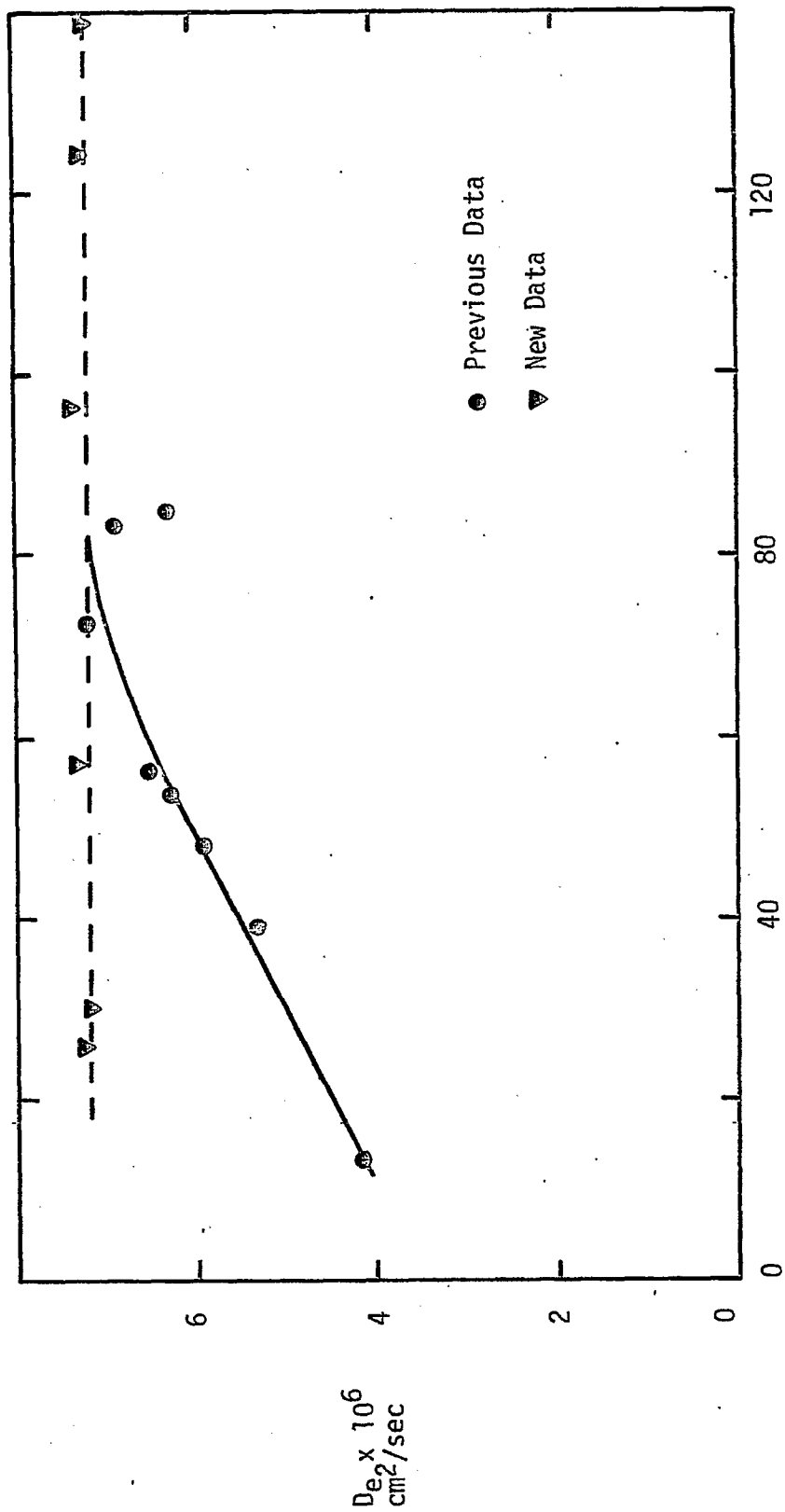
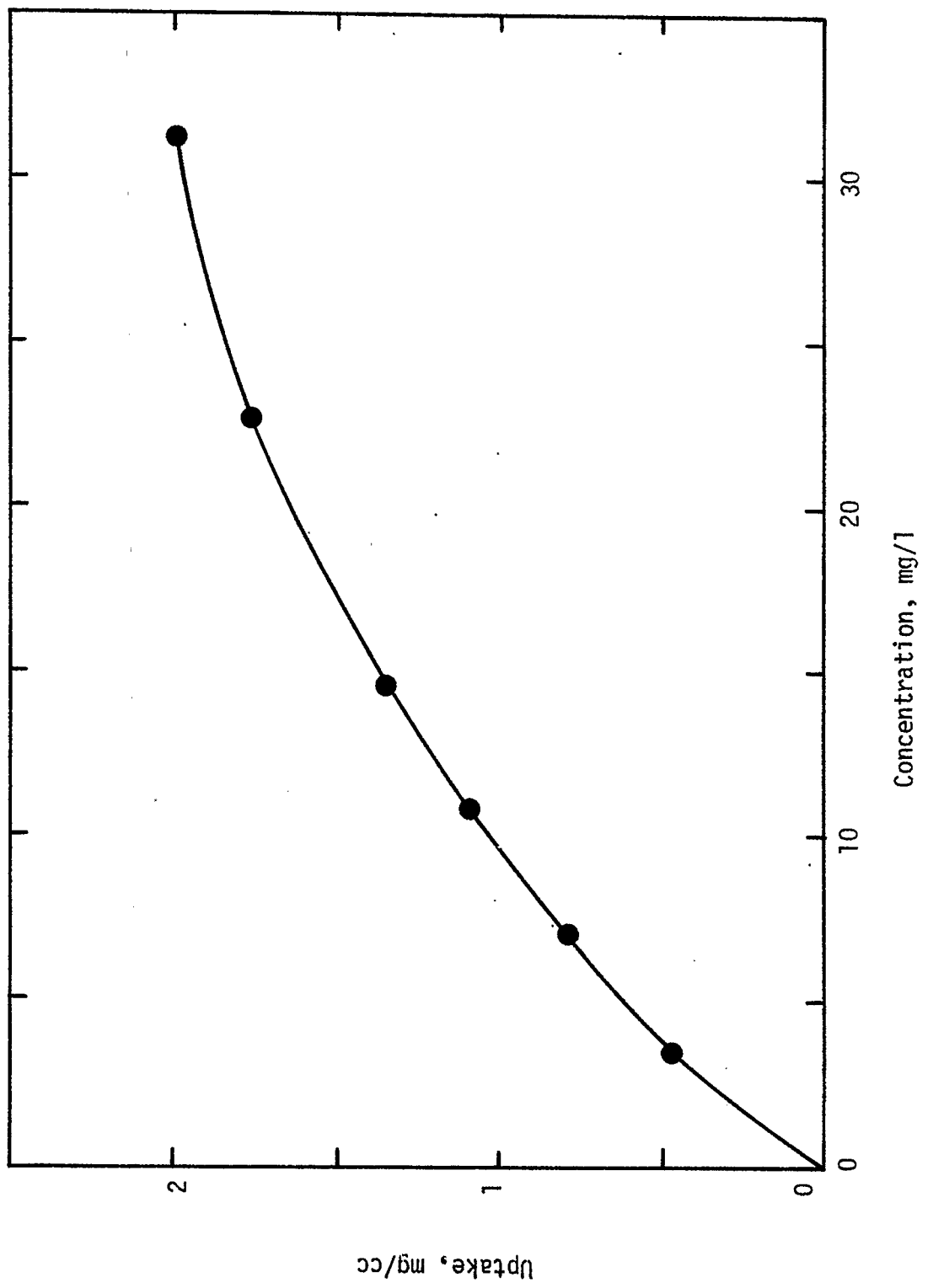


Figure 1. Effective Diffusivity vs. Adsorption Constant for Naphthalene in Cyclohexane with Catalyst L.

Figure 2. Adsorption isotherm of Naphthalene/cyclohexane with Catalyst L (500°C).



Task 13

Catalyst Research and Development

Faculty Advisor: A.G. Oblad
F.V. Hanson
Graduate Student: C.S. Kim

Introduction

The objectives of this project are to develop a preparation technique for a Raney Type catalyst (particularly Raney iron-manganese catalyst) and to find the optimum operating process variables for the maximum production of C₂-C₁₀ hydrocarbons via hydrogenation of carbon monoxide. Previous work has shown that promoted iron catalysts particularly those promoted with manganese are very promising for the production of C₂-C₁₀ hydrocarbons. The objectives of this investigation can be subdivided as follows:

1. Preparation of Raney type catalyst of various compositions, particularly Fe-Mn catalyst.
2. Establish catalyst characterization procedures which can be correlated with yield and selectivity parameters. The characterization procedures will include atomic adsorption, X-ray diffraction, BET surface area measurement, chemisorption, TGA and surface spectroscopic analysis such as ESCA, Auger, etc.
3. Investigate the effect of fixed bed process variables such as temperature, pressure, space velocity and H₂/CO ratio on yield and selectivity.
4. Study the interactions between the major catalyst component and promoters in terms of yield and selectivity to C₂-C₁₀ products.
5. Study the overall kinetics of carbon monoxide hydrogenation process.

A fixed bed reactor system was designed and construction was initiated with available materials. An extensive literature survey has been done on the preparation of Raney type catalysts.

Project Status

The construction of the fixed bed reactor system has been completed. A detailed schematic flow diagram is shown in Figure 1. The fixed bed reactor consists of a 20 inch long 316 stainless steel tube with a 1 inch O.D. and 1/2 inch I.D. and is embedded in a 3/4 inch thick aluminum block to enhance the uniform temperature distribution along the reactor tube. The reactor is positioned vertically, rather than horizontally, to minimize the possible entrainment of high molecular weight hydrocarbon products from the reaction in the reactor.

The reactant gas, a CO and H₂ mixture, will be dried and treated with activated carbon to remove any trace of water and metal carbonyls. After

passing through the reactor, the product gas and vapors will pass through Trap I and Trap II. Trap I will be kept at 100°C to remove the high boiling point hydrocarbons, while Trap II will be kept at 0°C in an ice bath to condense the low boiling point products, mainly water and alcohols. The remaining gas will pass through a Grove back pressure regulator, which will reduce the gas pressure to atmospheric pressure. The flow rate of the exit gas will be monitored by a dry testmeter. A gas chromatograph will analyze the composition of the exit gas.

The fixed bed reactor system has been tested for leaks and is now ready for use.

Future Work

A technique for the preparation of Raney iron-manganese catalyst will be developed. The following procedure for the preparation of Raney type catalyst will be used: 1) fusion of alloys, 2) size reduction, 3) decomposition of alloys by caustic solution and 3) washing of the remaining active components. Since Raney type iron-manganese catalysts (or alloys) are not commercially available, the above procedure will be used. Guidelines from the literature survey on the preparation of other types of Raney catalysts will be used. The hydrogenation of carbon monoxide will be studied after the catalysts are prepared.

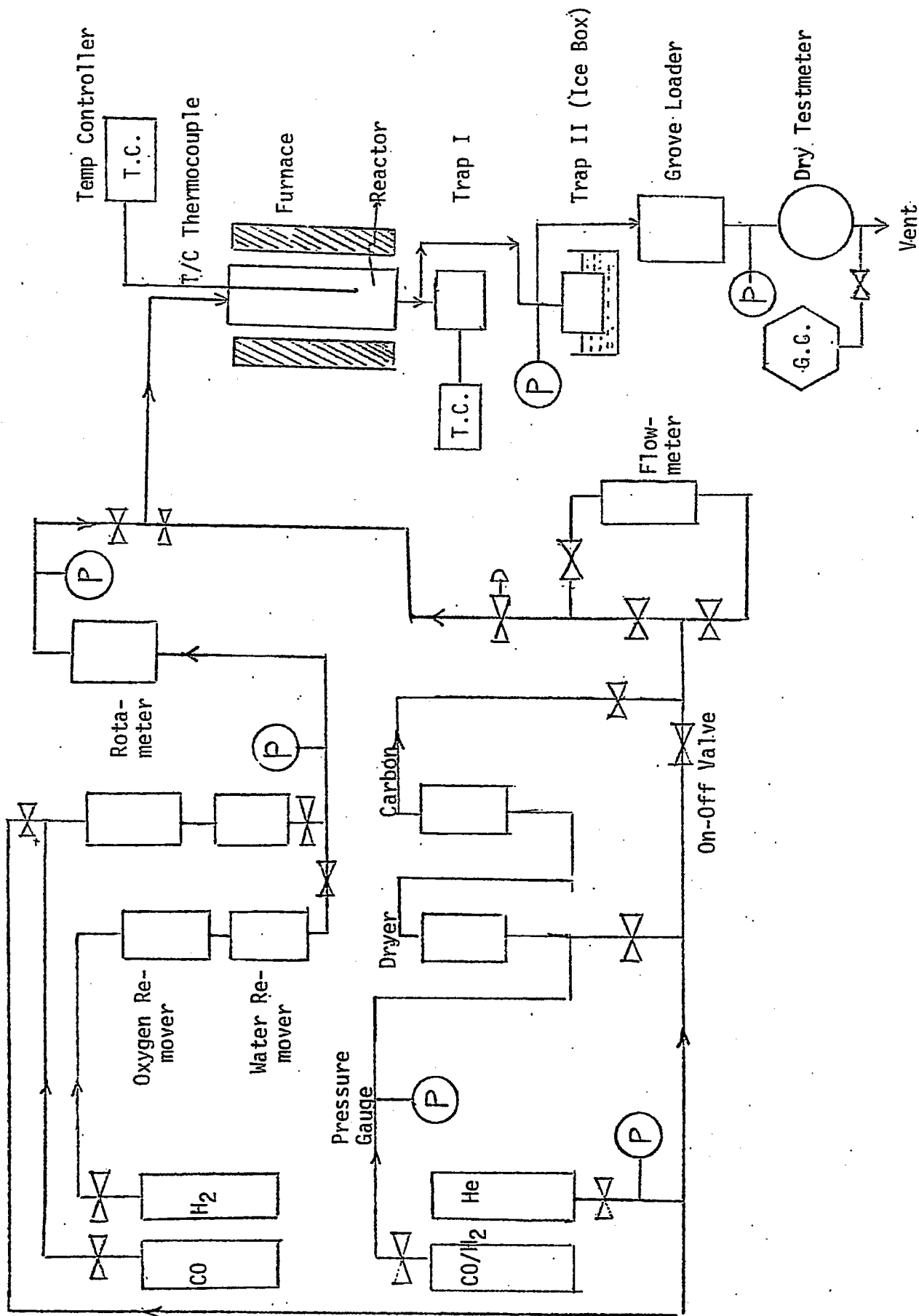


Figure 1. Flow Diagram of A Fixed Bed Reactor.

Task 14

Characterization of Catalysts and Mechanistic Studies

Faculty Advisor: F.E. Massoth
Graduate Student: K.B. Jensen

Introduction

This phase of the project is intended to supplement the high pressure reactor studies by detailed examination of the catalyst properties which enhance catalyst activity and selectivity. This is accomplished by characterization studies performed on fresh catalysts and on the same catalysts which have been run in the reactor. Of particular interest are metal areas, phase structure, catalyst stability and surface characteristics. Also, variables in catalyst preparation and pretreatment are examined to establish their effects on catalyst properties. Finally, in-situ adsorption and activity are studied under modified reaction conditions with a number of well-characterized catalysts to obtain correlating relationships.

The catalysts under present investigation are iron based catalysts promoted with manganese oxide.

Project Status

Some initial runs with the temperature-programmed desorption/reaction (TPD/TPR) apparatus were performed on reduced iron, manganese oxide and an iron manganese oxide catalyst (T9) containing 17.7 Mn/100 Fe. In these runs, there has been a problem with small amounts of oxygen contamination from the helium used, but action will be taken to eliminate this problem. A number of useful observations were made, however, and in some runs the oxygen contamination effects are minimal.

Figure 1 shows the result of a TPR experiment in a 2% CO in He mixture over a reduced iron catalyst. The CO concentration began to decrease around 200°C, indicating CO adsorption. At somewhat higher temperatures, CO₂ appeared which may have come from CO disproportionation or reaction of CO with contaminant oxygen on the catalyst. At higher temperatures, CO began to rise together with CO₂, going through a maximum. The increase in the CO may have been due to some CO desorption, whereas the peak in the CO₂ most likely was due to reaction of CO with contaminant oxygen. On holding the temperature at 500°C for one-half hour, both CO and CO₂ reached a steady state, indicating disproportionation was occurring since any oxygen contamination should have been removed by then.

The TPD/TPR experiments on pure MnO were less ambiguous than those performed on iron except for CO adsorption. Figure 2 shows the TPD of several preadsorbed gases. The oven dried catalyst was first reduced in H₂ at 500°C overnight. After purging with He the desired gas was exposed to the catalyst at room temperature for at least 15 minutes.

Helium was again introduced until the adsorbed gas concentration decayed to a stable value. The catalyst temperature was then raised linearly and the off gas monitored by the mass spectrometer. The catalyst was exposed to H_2 at $500^\circ C$ between runs. Carbon dioxide desorbs off the catalyst at around $210^\circ C$. Nitrogen and hydrogen showed no desorption peaks and therefore exhibited no adsorption on MnO . Carbon monoxide (2.2% in He) did not seem to adsorb on the MnO catalyst in one run, possibly due to preadsorbed oxygen blocking adsorption sites or too low a partial pressure of CO. A subsequent experiment in the microbalance, however, showed that pure CO can be adsorbed and desorbed from pure MnO with no net weight gain, indicating dissociative adsorption did not occur.

One carbon monoxide TPD run was done on Catalyst T9. A broad, shallow peak of carbon monoxide was formed at low temperature, as shown in Figure 3. Additional work will be needed to evaluate this result in perspective with studies on the pure iron catalyst.

The X-ray diffraction patterns of a number of used catalyst were examined. The main phases were iron and manganese oxide as had been previously found on freshly reduced catalysts. However, there is some evidence of carbide formation. The peaks of interest are very close to those of α -iron and make analysis difficult. Trends in apparent carbide peak heights with catalyst composition show no clear relationship. Iron catalysts are known to produce iron carbides during Fischer Tropsch synthesis.^{1,2} The catalysts that were used in the reactor studies had been exposed to synthesis gas at 500 psi and $200-260^\circ C$ for approximately 8 hours. Though a carbide phase appears evident, it seems to be less than 10%. Further experiments in the microbalance along with X-ray diffraction studies will be needed to describe and analyze what effect manganese oxides may have on carbide formation.

Future Work

The microbalance will be used to monitor the catalyst weight changes resulting from chemisorption of gases and carbon formation during H_2 -CO reaction. Samples will be analyzed by X-ray diffraction at various stages of reaction for carbide formation. The TPD/TPR runs will be continued with the mixed iron catalysts.

References

1. L.J.E. Hofer, E.M. Cohn and W.C. Peebles, J. Amer. Chem. Soc., 71, 189 (1949).
2. G.H. Barton and B. Gale, Acta Crystallogr., 16, 202 (1964).

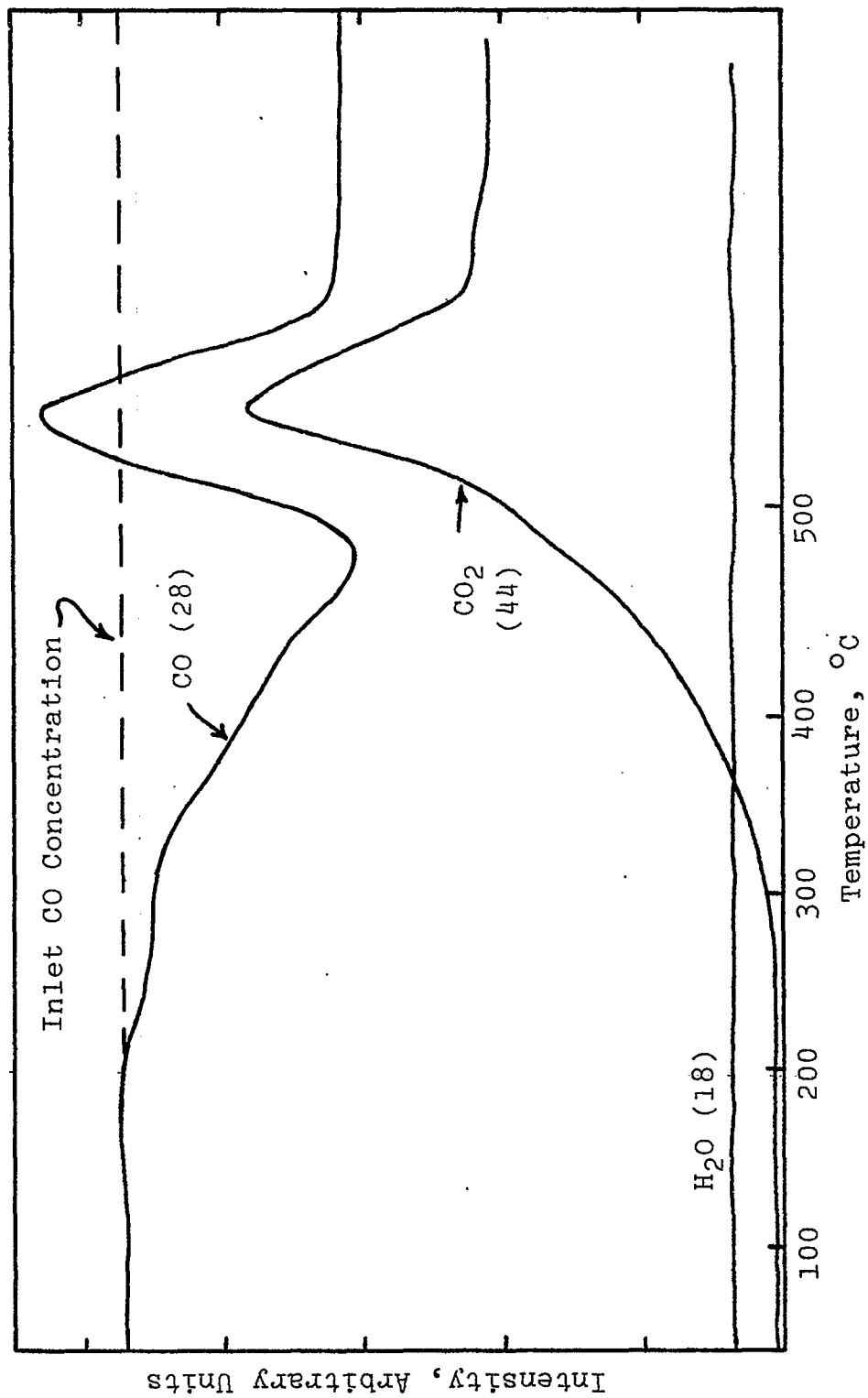


Figure 1. TPR of CO on Iron Catalyst 2.2% CO in Helium Mixture.

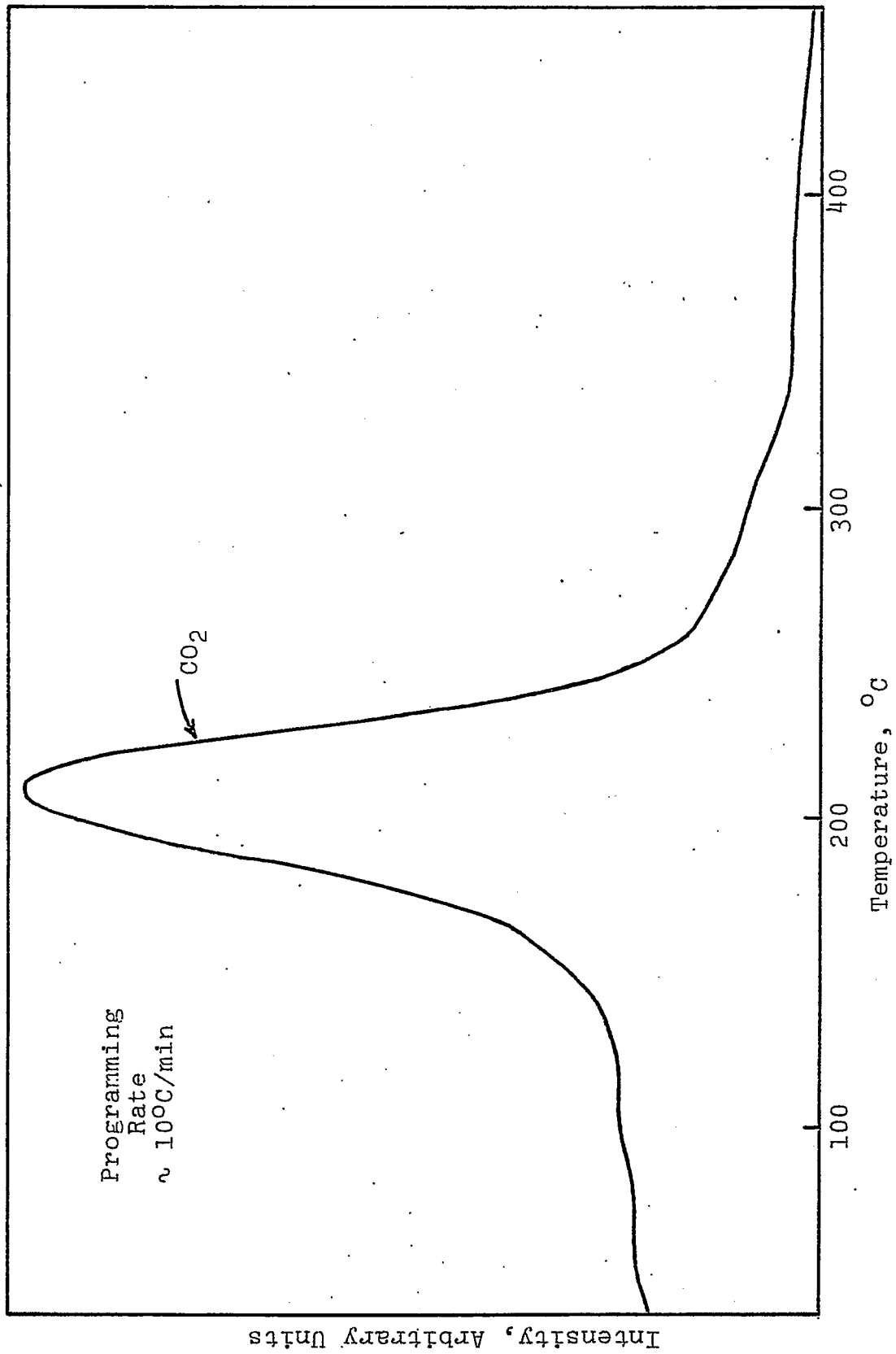


Figure 2. TPD in Helium of Preadsorbed CO₂ on MnO.

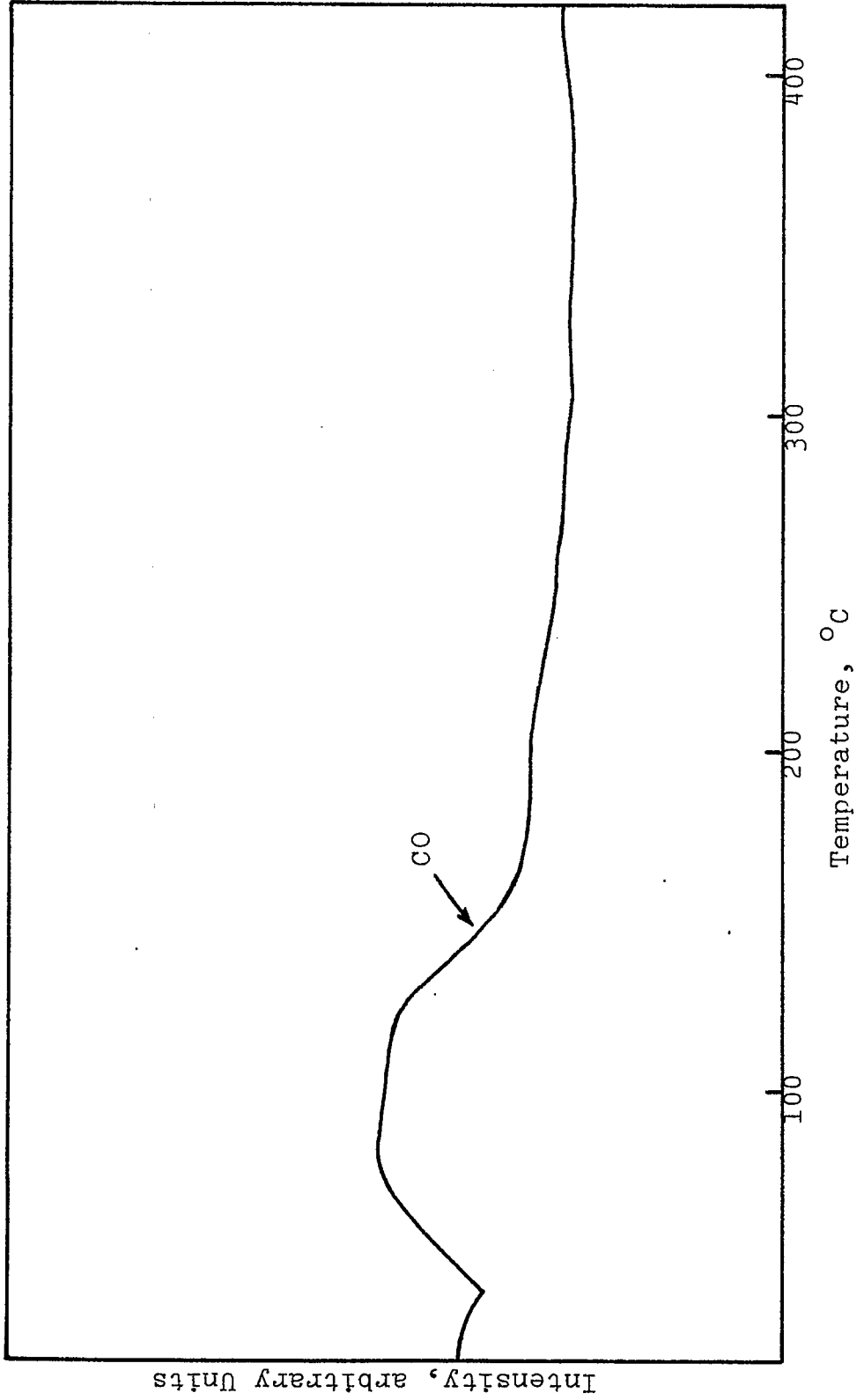


Figure 3. TPD in Helium of Preadsorbed CO on Catalyst T9.

V. Conclusions

Conclusions for each task are included in the individual reports. Task 9 did not have a student during this quarter and no work was done on Task 15.